The Thermal [2+2] Cyclodimerisation of (*E,Z*)-Cycloocta-1,3-diene Revisited − Chemical Trapping and Properties of the Intermediate 1,4-Diradicals

Johannes Leitich,*[a] Ingeborg Heise,[a] Klaus Angermund,[b] and Jörg Rust[b]

Dedicated to Professor William v. E. Doering on the occasion of his 85th birthday

Keywords: Cycloaddition / Radicals / Reaction mechanisms / Thermochemistry

The thermal [2+2] cyclodimerisation of (*E,Z*)-cycloocta-1,3-diene (**9**), which is known to afford the cyclobutane dimers **11**, **12**, and **13**, has been investigated in the presence of the nitroxyls **17** and **18** and of atmospheric dioxygen, all of which are known to be efficient trapping agents for carbon-centred free radicals. The nitroxyls have been found to divert the reaction from formation of the dimers to formation of 2:2 adducts of two molecules of **9** and two molecules of nitroxyl. The rate constant for the formation of the overall sum of the dimers plus the 2:2 adducts in the presence of nitroxyl has been found to equal the rate constant for the formation of dimers in the absence of nitroxyl. This and the molecular structures of the 2:2 adducts prove that two molecules of **9** combine irreversibly to produce the two epimeric bis(allylic) 1,4-diradicals **14** and **15** (*meso* and *rac*, respectively) which undergo two competing reactions: ring-closure to dimers **11**, **12**, and **13**, and trapping by nitroxyl to form the 2:2 adducts. Dioxygen, too, was found to trap **14** and **15** efficiently. From the kinetics of the latter trapping reaction, studied at six temperatures between 5 and 55 °C, the heights of the activation barriers separating **14** from **11** and **15** from **12** + **13** were estimated at 11.1 ± 1.5 and 10.2 ± 1.5 kcal·mol^{-1}, respectively, corresponding to diradical lifetimes of ca. 0.5 μs. These unexpectedly high barriers have been verified by MM3 force-field calculations and by an investigation of the kinetics of the gas-phase thermolysis of **12** (to give **13** and **16** which is an epimer of **12** and **13**) and of **13** (to give **12** and **16**). When the cyclodimerisation of **9** was carried out in the presence of spin = 1/2 transition metal complexes, no trapping was observed, but a shift in the **12**/**13** ratio, resulting from a catalysed conversion of **15** from its singlet to its triplet spin state, was seen. Since nitroxyl also catalysed the singlet-to-triplet conversion (dioxygen did not) in competition with trapping, the kinetics of trapping by nitroxyl was complex, but it did show that **14** and **15** were jeopardised to trapping twice in their lifetimes, meaning that **14** and **15** were generated in their *anti* conformations, which had to change to the *gauche* conformations by crossing the barriers referred to above before they could ring-close to dimers; all the *anti* and the triplet *gauche* conformations are trappable, but the singlet *gauche* conformations are not. The same conclusion was reached for **15** from independent experimental evidence. In addition, there is a minor path from **9** to dimers **11**, **12**, and **13**, which is not subject to trapping and which involves the direct formation of the singlet *gauche* conformers of **14** and **15** from **9**. The *gauche* conformer formed in the smallest amount along this minor pathway is the one giving rise to **12**, which is the one with its two radical p-orbitals pointing towards each other most strongly, thus causing adverse Woodward–Hoffmann effects. The direct formation of the principal *gauche* conformer (which gives rise to **13**) from **9** requires 2.75 ± 0.44 and 2.57 ± 0.42 kcal·mol^{-1} more activation energy than required for the formation of the *anti* conformers of **14** and **15**, respectively.

Introduction

According to a wealth of circumstantial evidence, thermal [2+2] cyclodimerisations of simple olefins to form cyclobutanes occur via 1,4-diradicals or 1,4-diradical-like species (referred to for simplicity as 1,4-diradicals in this section) in their singlet spin states (Scheme 1).[1] Singlet tetramethylene, which is the parent singlet 1,4-diradical (Scheme 1), has been prepared by a different route by pulse photolysis and has been shown to possess a lifetime of ca. 0.7 ps,[2,3] too long for a mere transition state. Hence, singlet 1,4-diradicals, if occurring in the course of [2+2] cyclodimerisations, should be intermediates rather than transition states. High-end theoretical calculations on singlet tetramethylene[3−7] revealed two species (*gauche* and *anti*, Scheme 1) without energy minima on broad, flat energy hypersurfaces, with surrounding barriers of between 0 and 3 kcal·mol^{-1} (Scheme 1). Though not protected by energy barriers, the *gauche* conformation is entropically protected and possesses a calculated lifetime about the same as that

[a] Max-Planck-Institut für Strahlenchemie,
Postfach 101365, 45413 Mülheim an der Ruhr, Germany
Fax: (internat.) + 49-208/306-3951
E-mail: leitich@mpi-muelheim.mpg.de
[b] Laboratorium für Chemische Kristallographie, Max-Planck-Institut für Kohlenforschung,
Kaiser-Wilhelm-Platz 1, 45470 Mülheim an der Ruhr, Germany
Fax: (internat.) + 49-208/306-2980
E-mail: lehmann@mpi-muelheim.mpg.de

found experimentally.[5] Two reaction paths ("1" and "2" in Scheme 1) for cyclodimerisation through 1,4-diradicals are conceivable: "1", involving the *anti* conformer of the 1,4-diradical, and "2", not involving it. The low or non-existent barriers found by the theoretical calculations suggest that there should be no strong preference for either path in the parent case of tetramethylene.

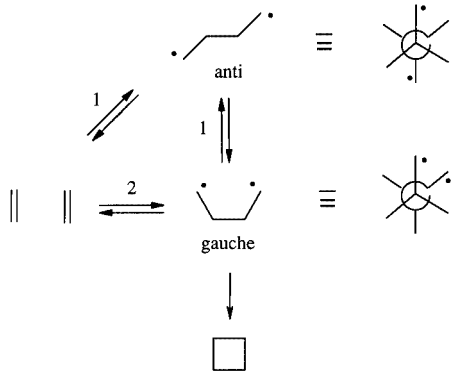

Scheme 1

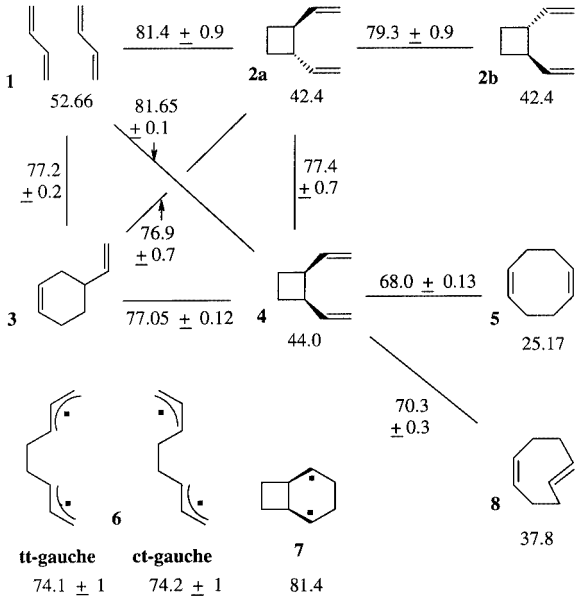

Heats of formation (kcal/mol) for C_8H_{12} isomers and transition states

Scheme 2

The head-to-head thermal [2+2] cyclodimerisation of 1,3-dienes through 1,4-diradical intermediates should enjoy an energy bonus of twice the stabilisation energy for allyl radicals (ca. 13.5 kcal·mol^{-1} [8]), about 27 kcal·mol^{-1} relative to simple nonconjugated olefins. Accordingly, 1,3-butadiene has been found to form only 1,2-divinylcyclobutanes (i.e., head-to-head) thermally, with no 1,3-divinylcyclobutanes being produced. Scheme 2 displays the experimentally determined heats of formation for 1,3-butadiene and various butadiene dimers and for the transition states[9] for the thermal interconversions between them.[10] Scheme 2 is an updated version of an earlier scheme by Doering and co-workers[11–13] and takes recalculated or more recent measurements into account.[14] Scheme 2 also displays two bis(allylic) 1,4-diradicals **6** that should be intermediates en route from butadiene to the 1,2-divinylcyclobutanes **2** and **4**; their heats of formation have been calculated from the heats of formation of the 1-methylallyl radicals[22] and from group increments.[15,23] The heat of formation for the bicyclic 1,4-diradical **7** also shown in Scheme 2 was calculated by MM3 force-field techniques.[24–27] The transition states for the two Cope rearrangements **4** $\rightleftarrows$ **5** and **4** $\rightleftarrows$ **8** are both energetically below all these diradicals (Scheme 2), in line with concerted mechanisms. All other transition states in Scheme 2, however, for which reactions involving **7** are out of question for chemical reasons, are energetically significantly higher than **6**, in line with reaction mechanisms involving **6**. The excess energies by which they are higher may partly represent potential energy barriers separating **6** from reactants, and may partly have a dynamic origin (i.e., some additional kinetic energy on top of a barrier may be necessary to move across it). The latter interpretation may find support in the higher activation energy required for **2a** $\rightleftarrows$ **2b** (in which two allyl groups must be rotated) as compared to **2a** $\rightleftarrows$ **4** (in which only one allyl group has to be rotated).

One particular point to be stressed is the particularly high barriers (81.5 ± 2 kcal·mol^{-1}) separating 1,3-butadiene (**1**) from the 1,2-divinylcyclobutanes (**2** and **4**); that is, for the [2+2] cyclodimerisation of **1**. Since two paths – "1" and "2" in Scheme 1 – are available for this cyclodimerisation and in view of the much lower barriers between **2**, **3** and **4**, this means that the barrier between **1** and **6**, even when allowing 2 kcal·mol^{-1} for excess kinetic energy (vide supra), must be more than 3.3 kcal·mol^{-1} higher than **6**,[28] and that the same applies either to the barrier between **1** and the *anti* conformer of **6** or to the barrier between the latter species and **6**.[29] In conclusion, there is a significant barrier between **1** and **6**, probably markedly higher than the analogous barrier in the case of tetramethylene.

A particular case of a thermal [2+2] cyclodimerisation of a 1,3-diene is that of (*E*,*Z*)-cycloocta-1,3-diene (**9**; Scheme 3), the title reaction. This proceeds even at room temperature, due to the high strain[16] in this diene. The reaction was discovered by Bloomfield and McConaghy,[30] who found that at sufficiently high concentrations of **9**, three dimers were formed besides the unimolecular rearrangement product of **9**, the already known **10**.[31,32] Padwa and co-workers assigned the molecular structures **12**, **13**, and **16** to the dimers;[33] structure **16** for the main dimer was later revised by Wiseman and Liu, who established the correct structure **11** by X-ray crystallography.[34,35] We have also verified the correct structure **11** by an alternative route (see below). The formation of **11**, **12**, and **13** is in line with the head-to-head regiospecificity pointed out in the preceding paragraph and with the intermediacy of diradicals **14** and **15**. However, there is an unanticipated stereoselectivity; the formation of **11**, **12**, and **13** corresponds to exclusive *trans* ring-closure of diradicals **14**

and **15**. A straightforward explanation for this remarkable stereoselectivity was afforded by the diradical hypothesis.[34,35] The conformations of the rather rigid eight-membered rings in **14** or **15** are necessarily such (see Figure 1) that the axes of the two allylic p-orbitals involved in the closure of the cyclobutane ring are both almost at right angles (more precisely, at 67.8° and 64.4°, respectively, according to MM3 calculations) to the axis of the central bond connecting the two rings. The ring-closing movement (which involves the mutual approach of the two reacting p-orbitals by a rotation of the central bond connecting the two rings) will therefore necessarily give rise to an overlap of the two p-orbitals that is stereochemically *trans*, no matter which *gauche* conformation of **14** or **15** is involved (Scheme 4). While (neglecting chirality) there is only one *gauche* conformer for **14**, there are two for **15**, one of which (**15*g*12**) would close to give **12**, and the other (**15*g*13**) to give **13**. Since both **12** and **13** are orbital-symmetry-forbidden products of a concerted dimerisation of **9**,[36,37] the virtually exclusive formation of **12** and **13** means that the two-step reaction via **15** does not show even the slightest orbital-symmetry-control effect.[34,35] Conformations **15*g*12** and **15*g*13** are separated from the *anti* diradical **15*a*** by rotational barriers, **15*ag*12** and **15*ag*13**, respectively, analogous to the *anti-gauche* (4.18 kcal·mol^{-1} calculated by MM3) and *gauche-gauche* (6.92 kcal·mol^{-1} calculated by MM3) barriers, respectively, in 2,3-dimethylbutane. As Wiseman and Liu point out,[34,35] this − plus the fact that **12** and **13** are formed in about a 4.5:1 ratio − suggests (albeit does not prove) that **15*g*12** and **15*g*13** might have been formed via **15*a***; in other words, it suggests a [2+2] cyclodimerisation via the *anti*-1,4-diradical.

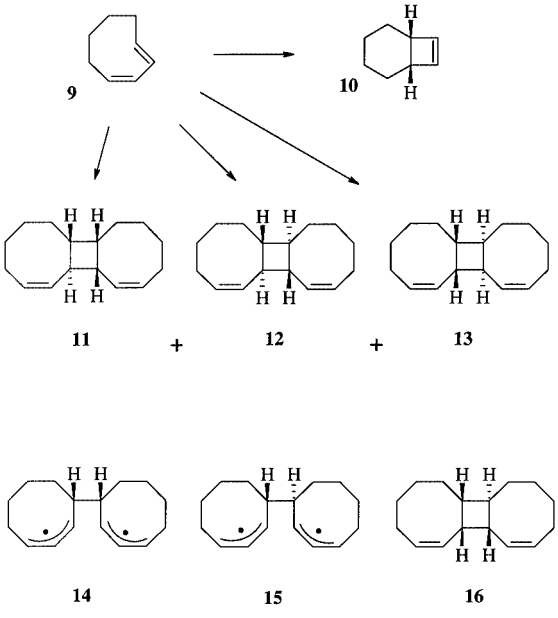

Scheme 3

Various types of singlet diradicals have been identified by chemical trapping as intermediates representing energy minima for numerous systems other than [2+2] cyclodimerisations, particularly by W. R. Roth and his coworkers.[38−41] For [2+2] cyclodimerisation of olefins and 1,3-dienes, in contrast, in spite of the large body of evidence

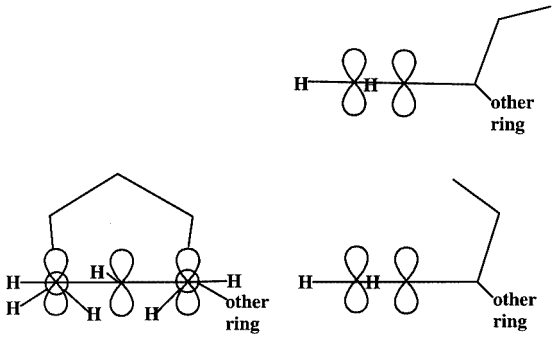

Figure 1. Front view (left) and side view (right) of the two lowest-energy eight-membered ring conformations in diradicals **14** and **15**; the front view is the same for either conformation; the top conformation (chair) is about 1.7 kcal·mol^{-1} higher in energy than the one (boat) at the bottom (MM3 calculations); "other ring" designates the position of attachment of the second eight-membered ring

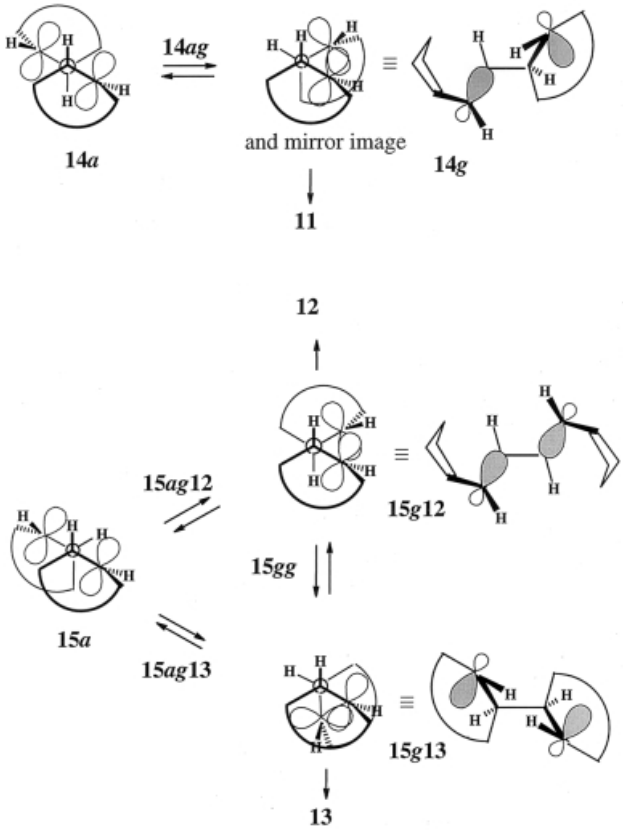

Scheme 4. Conformations (rotamers about the central bond) of diradicals **14** and **15**; in the left-hand and center views, the central bond connecting the two rings is vertical to the drawing plane; the ring above the drawing plane (bold face) is kept fixed in space while the other ring, below the drawing plane, is rotated; the right-hand views are at right angles to the center views, viewing the center objects from the right (**14*g*** and **15*g*12**) or lower right (**15*g*13**) sides; in the right-hand views, the orbital lobes pointing towards the viewer have been exaggerated in size; they have been shaded to indicate that the ring closure will occur between them; **14*ag***, **15*ag*12**, **15*ag*13** and **15*gg*** represent barriers between rotamers

that convincingly supports the diradical mechanism, none of the hypothetical singlet 1,4-diradical intermediates has so far been verified by spectroscopic observation or by chemical trapping. As a consequence, it had never been quite clear whether the two C−C bond-forming steps in [2+2] cyclodimerisations were strictly separated from each other in time, or whether there was some overlap between them in time, in other words, whether the intermediate was a "full-fledged" 1,4-diradical or whether it was merely a 1,4-"diradicaloid". Another hitherto unresolved question concerned the relative importance of reaction paths "1" and "2" (Scheme 1). Below, we wish to report on a reinvestigation of the title reaction that did result in successful trapping of the intermediate 1,4-diradicals **14** and **15** and, thanks to this trapping, in some knowledge about these diradicals and about the reaction mechanism.

Results and Discussion

Dimerisation of 9

Thermal dimerisation of **9** at ambient temperatures gave the three dimers **11**−**13**, as reported by the previous investigators.[33−35] According to GLC analysis, the dimer **16** (for synthesis, see below), the *cis* ring-closure product of **15**, was present in the crude dimer mixture of **9** at a level of only 0.11%, corresponding to a *trans*/*cis* closure ratio for **15** of 240. We also found (by catalytic hydrogenation of the crude dimer mixture and quantitative GLC analysis with known reference compounds[42]) that the two *cis* ring-closure products of **14** were present at levels of only 0.04 and 0.05%, respectively, corresponding to a *trans*/*cis* closure ratio for **14** of as much as 810, a remarkable stereoselectivity indeed (vide supra, Introduction section). Compound **10** was formed as a by-product at rates [in *n*-octane: $\log(A \times s) = 13.69 \pm 0.67$, $E_A = 28.33 \pm 0.94$ kcal·mol^{-1}] as reported by the earlier investigators.[30] No further products − and in particular no (*Z*,*Z*)-cycloocta-1,3-diene − were observed in the absence of catalytic effects; no polymers were formed in the presence of small amounts of inhibitors. Table 1 displays the kinetic results obtained for the dimerisation in *n*-octane in the temperature range 5−55 °C.[43] The dimerisation kinetics were second order in [**9**] in the concentration range 0.136−1.33 M. From the rate constants for the formation of the main dimer **11**, the Arrhenius parameters $\log(A \times s \times M) = 5.80 \pm 0.24$ and $E_A = 16.07 \pm 0.33$ kcal·mol^{-1}were obtained for the formation of **11** from **9** in *n*-octane (Figure 2). In dimethylformamide, which is drastically more polar than *n*-octane, very similar dimer ratios were found at all temperatures, together with fairly similar kinetic values for **11**, $k_{25\,°C} = (3.2 \pm 1.3)\times10^{-7}$ M^{-1}s^{-1}, $\log(A \times s \times M) = 6.7 \pm 1.7$, $E_A = 18.0 \pm 2.5$ kcal·mol^{-1}. For **12** + **13**, the Arrhenius parameters were quite similar to those for **11**.[44]

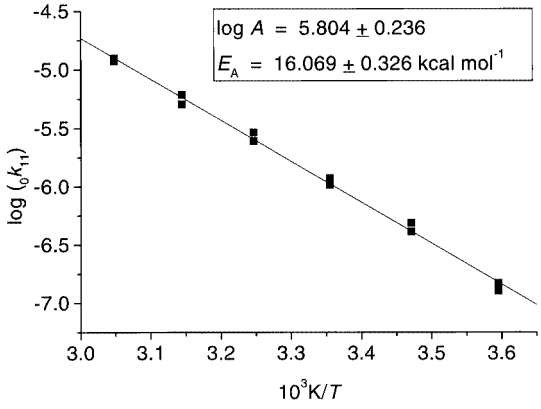

Figure 2. Arrhenius plot of the bimolecular rate constants for the formation of dimer **11** from **9** in *n*-octane

Dimerisation of 9 in the Presence of Nitroxyls (R_2NO·), Part 1

While the dimers were produced from **9** in similar proportions and at similar rates in all common solvents at room temperature, an entirely different result was obtained when di-*tert*-butylaminooxyl (**17**) was used as the solvent. One main product, **19b***u***19b** (Scheme 5), a 2:2 adduct of two molecules of **9** and two molecules of **17**, crystallised from the reaction mixture, with the remainder consisting of isomers of **19b***u***19b** and only a small amount of dimers **11**−**13**. With TEMPO (**18**) in place of **17**, the result was analogous; Table 2 shows the product composition obtained with **18**. The composition of the 2:2 adduct mixtures appeared independent of nitroxyl concentration. Solvent **17** differed from **18** in that it formed only very small amounts of 1:2 adducts of one molecule of **9** and two molecules of **17**, whereas with **18** these amounts were substantial (Table 2). Solvents **17** and **18** did not influence the formation of **10**, but did cause some catalytic conversion of **9** into (*Z*,*Z*)-cycloocta-1,3-di-

Table 1. Kinetic data for formation of dimers **11**−**13** from **9** in *n*-octane

T [°C][a]	*n*	[**13**]/[**12**]	[**11**]/([**12** + **13**])	$_0k_{11}\times s\times M\times10^7$	$_0k_{12}\times s\times M\times10^7$
5.1	8	0.191 ± 0.006	2.992 ± 0.040	1.37 ± 0.10	0.39 ± 0.02
15.0	4	0.216 ± 0.001	3.006 ± 0.016	4.47 ± 0.38	1.22 ± 0.02
25.0	7	0.218 ± 0.003	2.805 ± 0.029	11.07 ± 0.75	3.24 ± 0.02
35.0	7	0.207 ± 0.001	2.834 ± 0.065	26.85 ± 2.26	7.75 ± 0.77
45.0	7	0.188 ± 0.008	2.755 ± 0.045	55.84 ± 5.22	16.94 ± 1.46
55.1	6	0.164 ± 0.005	2.807 ± 0.012	122.17 ± 3.15	37.45 ± 1.00

[a] Under argon. For definition of *k* values see ref.[43] The subscript 0 indicates *k* values obtained in *n*-octane under 1 atm of argon in the absence of additives.

ene, which was noticeable at high nitroxyl concentrations (ca. 0.3 times the sum of dimer and 2:2 adduct formation at [**17**] = 1 M and [**9**] = 0.45 M). No polymer was formed.

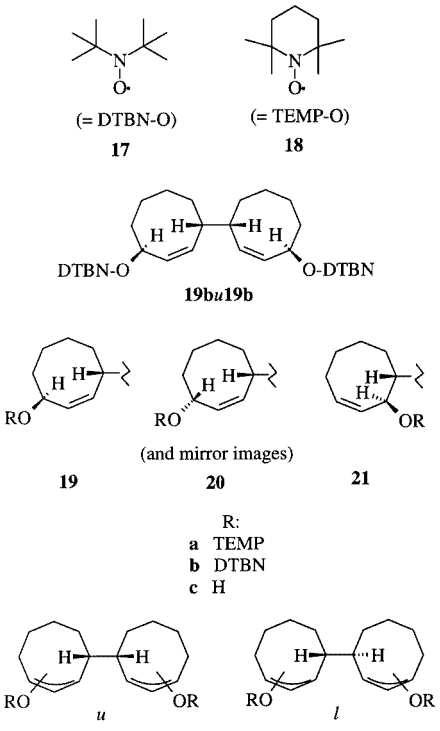

Scheme 5

Table 2. Product composition (as %; sum = 100; excluding **9**, **10**, and *Z,Z*-cycloocta-1,3-diene; 0.8 % of **9** remained unreacted) obtained from a 1:1.07 (mol/mol) mixture of **9** and **18** (= OR) after 13 d at room temp.

(2:2) adducts *u*		(2:2) adducts *l*		(1:2) adducts		(2:0) dimers	
19a*u*19a	63.8	**19a/19a**	8.9	**19a**OR	5.4	**11**	1.5
19a*u*20a	4.0	**19a/20a**	1.1	**20a**OR	0.5	**12**	0.4
19a*u*21a	2.2	**19a/21a**	6.7	**21a**OR	0.5	**13**	1.3
		21a/21a	0.7	miscellaneous			
				1.3[a]			
				1.7[b]			
Sum:	70.0		17.4	9.4			3.2

[a] (*Z,Z*)-5-RO-cycloocta-1,3-diene. [b] Mainly monooxygenated (2:2) adducts (MS analysis).

Scheme 5 and Table 2 show that all the 2:2 adducts possessed the $C_{16}H_{24}$ skeletons either of **14** ("*u*" in Scheme 5) or of **15** ("*l*" in Scheme 5). The relative amount of *u* products in Table 2 is 3.74 times that of *l* products, which compares with the amount of the *u* dimer **11** relative to that of the *l* dimers **12** + **13** when these dimers were formed in the absence of nitroxyls (2.8−3.0 in *n*-octane, Table 1; the difference between the values 3.74 and 2.8−3.0 may be due to a solvent effect). These facts strongly suggest that **17** and **18** had trapped diradicals **14** and **15** en route to dimers **11**−**13** to furnish the 2:2 adducts. Confirmation of this was afforded by the reaction kinetics. Table 3 presents the bimolecular rate constants for formation of dimers **11**−**13**, defined as the increase per second in the molar concentration (in terms of C_8H_{12} units) of dimers, divided by 2[**9**]^2, in the presence of **17**. These rate constants do not depend on [**9**], but strongly decrease with increasing [**17**]. Table 3 furthermore presents a second set of bimolecular rate constants, viz. the increase per second, divided by 2[**9**]^2, of the molar concentration (in terms of C_8H_{12} units) of the sum of dimers plus 2:2 adducts. These rate constants, in contrast to the former ones, depend (within the error limits) neither on [**9**] nor on [**17**] and are equal to the bimolecular rate constants for formation of dimers **11**−**13** in the absence of nitroxyls. This kinetic evidence establishes that in the rate-determining step two molecules of **9** combine irreversibly to form an intermediate, and that this intermediate undergoes two competing reactions, formation of dimers **11**−**13**, which in the absence of nitroxyls is the sole reaction, and reaction with nitroxyl to form the 2:2 adducts (Scheme 6). The $C_{16}H_{24}$ skeletons of the 2:2 adducts show that this intermediate must be either the 1,4-diradicals **14** and **15** or the corresponding 1,4-dipoles. The dipoles can be dismissed as a possibility since, firstly, fast addition to nitroxyls is a reaction typical of carbon-centred free radicals[45−48] but not of ions, and secondly, the rate of formation of the intermediate does not depend on solvent polarity (vide supra); the rates of [2+2] cyclodimerisations occurring via 1,4-dipoles, in contrast, increase by several orders of magnitude with solvent polarity.[49]

To the best of our knowledge, the current investigation is the first that has not only suggested but demonstrated the intervention of nonconjugated (between the two radical centres) 1,4-diradicals as true intermediates in the course of a thermal [2+2] cycloaddition[50−52] and thus demonstrated that this cycloaddition occurred by two strictly separated steps.

The presence of nitroxyls not only reduced the formation of dimers, but also changed their proportions. While in the absence of nitroxyls dimer **13** amounted to only ca. 4.7% of the dimer mixture (Table 1), in the experiment reported in Table 2 it constituted 40% of the dimer mixture. Plots of the rates of formation of individual dimers vs. [**17**]$^{-1}$ on extrapolation to [**17**]$^{-1}$ = 0 (i.e., to infinite nitroxyl concentration), suggested that at infinite nitroxyl concentration there remained small amounts of each dimer, the formation of which was uninfluenced by nitroxyl. These amounts constituted 1.5%, 2.5% and 26 ± 3%, respectively, of all **11**, **12** and **13** formed in the absence of nitroxyl, which translates into a proportion of "untrappable" dimers of **11/12/13** ≈ 38:19:42. In striking contrast to the "trappable" dimers, the "untrappable" ones are dominated by **13**.

The highly efficient trapping of the intermediate diradicals by nitroxyl in the course of the dimerisation of **9** raised the question of whether a comparable trapping might be observed with 1,3-butadiene and its dimers (Scheme 2). Preliminary experiments on the thermolysis of **2** in solution at 120 °C up to ca. 10% conversion revealed that the rates of formation of **3** and **5** were reduced by about one fifth and

Table 3. Observed rate constants for dimerisation of **9** in *n*-octane under argon at 25°C in the presence of varying concentrations of di-*tert*-butylnitroxyl (**17**); rate constants are changes of concentrations (M) of species in terms of C_8 units per second, divided by 2[**9**]^2; k_{dim} = observed rate constants for formation of dimers **11** + **12** + **13**; $k_{deficit}$ = observed (by GLC) rate constants for the disappearance of the sum of **9** + **10** + (*Z*,*Z*)-cycloocta-1,3-diene + **11** + **12** + **13**, ≈ rate constant for formation of **17/9** = 2:2 adducts (no polymers and only minimal amounts of **17/9** = 2:1 adducts are formed)

[**17**]/M	0	0.038	0.1	0.19	0.38	0.59	1.16	2.37
[**9**]/M				$k_{dim} \times 10^7 \times$M×s				
0.235	14.3 ± 0.8	9.71 ± 0.46	6.04 ± 0.55	3.83 ± 0.32	2.18 ± 0.12	1.47 ± 0.06		
0.44				3.19 ± 0.22	1.86 ± 0.14	1.24 ± 0.04	0.83 ± 0.08	
0.73						1.29 ± 0.05	0.79 ± 0.14	0.57 ± 0.08
1.34				(k_{dim} + $k_{deficit}$) × 10^7×M×s		1.44 ± 0.10	0.87 ± 0.08	0.58 ± 0.07
0.235	14.3 ± 3.7	15.5 ± 4.5	14.2 ± 3.8	15.8 ± 5.6	14.5 ± 2.3	14.4 ± 2.6		
0.44	13.8 ± 2.7			14.4 ± 8.7	13.0 ± 4.5	12.4 ± 1.7	14.2 ± 3.3	
0.73	14.4 ± 4.0					12.3 ± 1.8	13.1 ± 1.5	13.8 ± 0.8
1.34	14.3 ± 3.7					12.8 ± 1.6	14.1 ± 0.5	14.9 ± 0.9

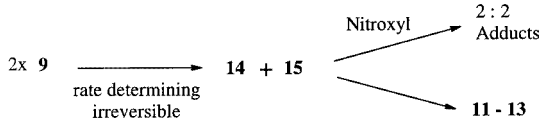

Scheme 6

one third, respectively, when the nitroxyl **18** was used as the solvent relative to when xylene was the solvent (after extrapolation to zero conversion since slow consumption of products by **18** was observed). Thus, although there is some trapping, it appears to be very much less efficient than in the case of **9**.

Dimerisation of 9 in the Presence of Atmospheric Oxygen

Like carbon-centred free monoradicals, which add $^3(O_2)$ (atmospheric oxygen) even more rapidly than they add nitroxyls, **14** and **15** are highly efficiently trapped not only by nitroxyls but also by atmospheric oxygen. This fact may easily escape notice; when, in a typical preparative experiment, non-agitated neat **9** was allowed to dimerise under ambient conditions, excellent yields of dimers were isolated no matter whether the dimerisation had been carried out under air or under argon. When, however, vigorously agitated dilute solutions of **9** were allowed to dimerise at ambient conditions under pure oxygen, analytically determined yields of **11** and **12** dropped dramatically to a few percent of what they had been if argon had been used in place of oxygen, even though the consumption of **9** was the same in either case. The discrepancy between the two sets of experiments was due to rapid depletion of oxygen in the reaction mixture for dimerisation of neat, non-agitated **9**, and this depletion was in turn due to a combination of the low saturation concentration of oxygen in liquids under ambient conditions, rather slow diffusion, and high dimerisation reaction rates. No attempt was made to isolate the products resulting from the trapping of **14** and **15** by oxygen. By taking suitable precautions to make sure the depletion effect was negligible, it was possible to perform kinetic studies of the dimerisation of **9** in the presence of oxygen in *n*-octane. These studies used the analytically observed rate constants for formation of the individual dimers under 1 atm of argon, of air, and of pure oxygen, respectively. The equilibrium concentrations of oxygen in *n*-octane under 1 atm of oxygen between 5 and 55 °C (Table 4, Column 2) were determined by a modified Clemens Winkler method. Assuming the trapping of **14** and **15** to be kinetically of first order with respect to oxygen, we can write

Table 4. Kinetic data on the trapping of diradicals **14** and **15** by O_2 in *n*-octane; $[O_2]_{sat}$ = saturation concentration of O_2 in *n*-octane under 1 atm of O_2; rate constants: k_{RC} for ring-closure of **14** to **11**, of **15** to **12** and of **15** to **13**, respectively; k_T = for trapping of **14** and **15**, respectively, by O_2; $_Uk$ for formation of untrappable **12** and **13**, respectively, from **9**; $_0k$ for formation of **12** and **13**, respectively, under argon in the absence of oxygen

1	2	3	4	5	6	7	8	9	10
T [°C]	$[O_2]_{sat}$ × mM^{-1} × atm	$_{11}k_{RC} \times 10^4$/ ($_{14}k_T \times$ M)	$_{12}k_{RC} \times 10^4$/ ($_{15}k_T \times$ M)	$_{13}k_{RC} \times 10^5$/ ($_{15}k_T \times$ M)	$_Uk_{13} \times 10^9 \times$ M × s	$_{11}k_{RC} \times 10^{-5} \times$ s	$_{12}k_{RC} \times 10^{-5} \times$ s	$_{12}k_{RC}$ / $_{13}k_{RC}$	($_0k_{12} - _Uk_{12}$)/ ($_0k_{13} - _Uk_{13}$)
5	13.25	1.165 ± 0.032	0.975 ± 0.056	0.83 ± 0.63	1.71 ± 0.06	5.497 ± 0.150	4.603 ± 0.262		7.05 ± 0.70
15	12.72	2.146 ± 0.109	1.930 ± 0.079	3.51 ± 0.77	6.21 ± 0.40	10.130 ± 0.516	9.108 ± 0.371	5.50 ± 1.23	6.05 ± 0.60
25	12.20	4.133 ±0.232	3.456 ± 0.165	2.76 ± 2.10	20.64 ± 0.54	19.51 ± 1.09	16.31 ± 0.78		6.49 ± 0.23
35	11.67	8.541 ± 0.125	6.251 ± 0.083	9.74 ± 0.47	47.07 ± 1.68	40.31 ± 0.59	29.50 ± 0.39	6.41 ± 0.32	6.67 ± 0.70
45	11.15	13.715 ± 0.687	9.492 ± 0.479	11.24 ± 0.83	135.80 ± 4.93	64.73 ± 3.24	44.80 ± 2.26	8.45 ± 0.76	9.13 ± 0.90
55	10.62	24.320 ± 1.763	17.036 ± 0.528	15.96 ± 1.54	318.70 ± 16.80	114.80 ± 8.32	80.41 ± 2.49	10.67 ± 1.07	15.5 ± 4.5

$$(k_{11} - {}_{U}k_{11})/({}_{0}k_{11} - k_{11}) = {}_{11}k_{RC}/({}_{14}k_{T} \times [O_2]) \quad (1a)$$

$$(k_{12} - {}_{U}k_{12})/[{}_{0}k_{12} + {}_{0}k_{13} - (k_{12} + k_{13})] = {}_{12}k_{RC}/({}_{15}k_{T} \times [O_2]) \quad (1b)$$

$$(k_{13} - {}_{U}k_{13})/[{}_{0}k_{12} + {}_{0}k_{13} - (k_{12} + k_{13})] = {}_{13}k_{RC}/({}_{15}k_{T} \times [O_2]) \quad (1c)$$

where k_{11} is the observed rate constant for formation of **11** in the presence of an oxygen concentration $[O_2]$, ${}_{0}k_{11}$ is the analogous rate constant observed under argon in the absence of oxygen, ${}_{U}k_{11}$ is the rate constant for formation of the untrappable **11**, ${}_{11}k_{RC}$ is the rate constant for ring-closure of **14** to form **11**, ${}_{14}k_{T}$ is the rate constant for trapping of **14** by oxygen, and the analogous quantities in Equations (1b) and (1c) have the same meaning for **12**, **13** and **15** in place of **11** and **14**. Equations (1a) to (1c) rearrange to

$$y_{11} = a_{11} + b_{11} \times x_{11} \quad (2a)$$

$$y_{12} = a_{12} + b_{12} \times x_{(12+13)} \quad (2b)$$

$$y_{13} = a_{13} + b_{13} \times x_{(12+13)} \quad (2c)$$

where y_{11}, y_{12} and y_{13} are the experimentally determined variables $k_{11}/{}_{0}k_{11}$, $k_{12}/({}_{0}k_{12} + {}_{0}k_{13})$ and $k_{13}/({}_{0}k_{12} + {}_{0}k_{13})$, respectively, x_{11} and $x_{(12+13)}$ are the experimentally determined variables $(1 - y_{11})/[O_2]$ and $(1 - y_{12} - y_{13})/[O_2]$, respectively, a_{11}, a_{12} and a_{13} are the constant parameters ${}_{U}k_{11}/{}_{0}k_{11}$, ${}_{U}k_{12}/({}_{0}k_{12} + {}_{0}k_{13})$ and ${}_{U}k_{13}/({}_{0}k_{12} + {}_{0}k_{13})$, respectively, and b_{11}, b_{12} and b_{13} are the constant parameters ${}_{11}k_{RC}/{}_{14}k_{T}$, ${}_{12}k_{RC}/{}_{15}k_{T}$ and ${}_{13}k_{RC}/{}_{15}k_{T}$, respectively. For each dimer at each temperature, linear regression according to Equations (2a) to (2c) was carried out. The values obtained for the three constant parameters *b* are presented in Table 4 (Columns 3−5). For **11** and **12**, the values obtained for *b* showed satisfactory precision (Columns 3 and 4) whereas the values obtained for *a* were too imprecise to differ significantly from zero and have not been included in Table 4. For **13** the situation is reversed; *b* values are rather imprecise (Column 5) but *a* values (Column 6, after multiplication by ${}_{0}k_{12} + {}_{0}k_{13}$) show good precision, which is due to *a* being much larger in case **13** than in cases **11** and **12**.

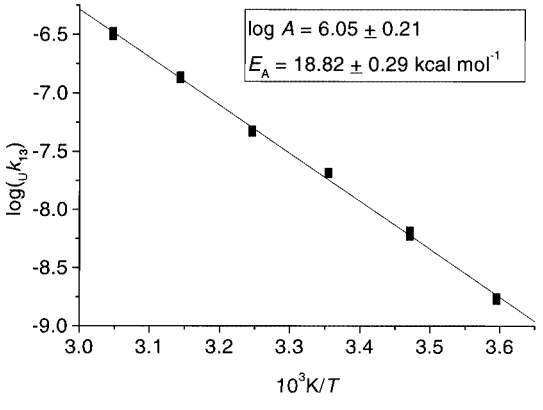

Figure 3. Arrhenius plot of the bimolecular rate constants for the formation of the untrappable fraction of dimer **13** from **9** in *n*-octane

The following conclusions emerge:

i. The value obtained for a_{13} at 25 °C translates into a fraction of 29.2 ± 2.1% of the total amount of **13** formed under argon being untrappable. This compares with the 26 ± 3% found with nitroxyl (vide supra), which shows that exactly those species that are untrappable by nitroxyl are also untrappable by oxygen. The values obtained for a_{11} and a_{12} correspond to < 3% of the total **11** and **12**, respectively, in line with the more precise values observed with nitroxyl (vide supra).

ii. The Arrhenius plot of the ${}_{U}k_{13}$ values (Column 6) is presented in Figure 3. The resulting Arrhenius parameters for the formation of untrappable **13** from **9** are $\log(A \times \text{M} \times \text{s}) = 6.05 \pm 0.21$ and $E_A = 18.82 \pm 0.29$ kcal·mol^{-1}.

iii. The ratios of b_{12} (Column 4) to b_{13} (Column 5) are presented in Column 9, except for two temperatures at which b_{13} was too imprecise. These ratios $({}_{12}k_{RC}/{}_{13}k_{RC})$ agree within the limits of precision with the ratios $({}_{0}k_{12} - {}_{U}k_{12})/({}_{0}k_{13} - {}_{U}k_{13})$ (Column 10). This shows that the values of ${}_{12}k_{RC}/{}_{13}k_{RC}$ remained unchanged by the presence of oxygen with respect to what they were under argon.

iv. The *b* values in Columns 3−5 of Table 4 could be converted into k_{RC} values if values for k_T were known. Rate constants for irreversible trapping of carbon-centred monoradicals in organic solvents by oxygen at 27 °C have been determined,[54] and were very similar to those determined in water.[55] Irrespective of solvent, they spanned the narrow range from 1.64×10^9 M^{-1}s^{-1} (for the most stabilised radical, cyclohexadienyl, in benzene) to 4.7×10^9 M^{-1}s^{-1} (for the least stabilised radical, methyl, in water) and 4.93×10^9 M^{-1}s^{-1} (for *tert*-butyl in cyclohexane). Of the radicals reported in these investigations, benzyl (stabilised similarly to allyl) was adopted as the closest model for **14** and **15**. As judged from allyl systems,[56] the reactions of benzyl, **14** and **15** with oxygen should be irreversible under our conditions. The value determined for benzyl was 2.36×10^9 M^{-1}s^{-1} in cyclohexane[54] (2.77×10^9 M^{-1}s^{-1} in water[55]). Twice this value (since **14** and **15** have two equivalent sites of attack), 4.72×10^9 M^{-1}s^{-1}, was adopted for **14** and **15** at 25 °C. Together with the b_{11} value (Column 3) for 25 °C, this value yields a ${}_{11}k_{RC}$ value of $(19.51 \pm 1.09) \times 10^5$ s^{-1}, corresponding to a lifetime of **14** of 513 ± 29 ns at 25 °C. No data on the temperature dependence of rate constants for trapping of free radicals by oxygen in solution appear to have been published so far. In the gas phase, in which studies have been made, rate constants increase only very slightly,[57] or even decrease slightly,[58−63] with temperature. The rate constants for quenching of aromatic triplet states by oxygen, a reaction mechanistically closely related to trapping of free radicals by oxygen, in solution at 5−55 °C also show only modest changes with temperature, some constants increasing, some decreasing.[64] It thus appeared that the assumption of k_{RC} being temperature-independent would not be too far off the truth. The k_{RC} values for **11** and **12** obtained on the basis of this assumption are presented in Table 4, Columns 7 and 8. The Arrhenius plot of the ${}_{11}k_{RC}$ values is shown in Figure 4. The resulting Arrhenius parameters for the ring-closure of **14** to form **11** are

$\log(A \times s) = 14.48 \pm 0.16$ and $E_A = 11.14 \pm 0.22$ kcal·mol^{-1}. Similarly, $\log(A \times s) = 13.70 \pm 0.14$ and $E_A = 10.21 \pm 0.19$ kcal·mol^{-1} are obtained for the ring-closure of **15** to form **12**; parameters similar to the latter, albeit much less precise, describe the ring-closure of **15** to form **13**. The inaccuracy introduced by the assumption of temperature independence can be estimated to increase the error limits of the E_A values to $\pm$ 1.5 kcal·mol^{-1}. The barriers separating **14** and **15** from **9** and from (*Z*,*Z*)-cycloocta-1,3-diene must be even higher than the above barriers, since formation of **14** and **15** from **9** is irreversible (vide supra) and since no (*Z*,*Z*)-cycloocta-1,3-diene is formed as a by-product of dimerisation in the absence of catalysis. Structures **14** and **15** therefore represent unexpectedly deep energy troughs.

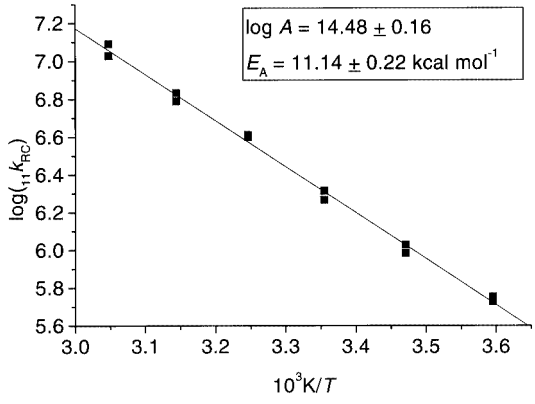

Figure 4. Arrhenius plot of the unimolecular rate constants for ring-closure of diradical **14** to form **11** in *n*-octane

Dimerisation of 9 in the Presence of other Radical Trapping Agents

The stable free radical galvinoxyl was found to be a very efficient trapping agent, similarly to nitroxyls, for **14** and **15**. No detailed investigation of this trapping reaction has been carried out, however. Thiols, bromotrichloromethane and tetrabromomethane differ from nitroxyl, galvinoxyl and dioxygen in that they are closed-shell compounds, but they are still known to be efficient trapping agents for carbon-centred monoradicals, which abstract one atom from them. With **14** and **15**, however, they were completely inefficient and did not influence the dimerisation of **9** even if, for example, ethanethiol was present as 50% of the solvent.

Thermolysis of 12 and 13; Force-Field Calculations

The high barriers (of ca. 11 and 10 kcal·mol^{-1}) that appear to protect the diradicals **14** and **15** against ring-closure contrast strikingly with the low barriers (of ca. 3 kcal·mol^{-1} [53]) that protect the diradicals **6** against ring-closure (Scheme 2). These unexpectedly high barriers invite verification by thermolysis experiments analogous to those indicated in Scheme 2 and also by MM3 force-field calculations.

The thermal interconversions indicated in Scheme 2, as well as those in the system of penta-1,3-diene and its dimers,[65] occur with reasonable rates at 140 °C; those in the system of 3-methylenecyclohexene and its dimers occur even below 100 °C.[53] In contrast, **12** and **13** required temperatures above 200 °C for thermolysis to become noticeable. Table 5 presents kinetic data on the gas-phase thermolysis of **12** and **13**, obtained at 220−260 °C and at conversions below 7%. Under these conditions, **12** was converted into **13** and **16**, and **13** was converted into **12** and **16**. From the rate constants in Table 5, the Arrhenius parameters $\log(A \times s) = 12.66 \pm 0.50$ and $E_A = 46.07 \pm 1.18$ kcal·mol^{-1} were obtained for the reaction **12** → **13**; for the reaction **12** → **16**, $\log(A \times s)$ was higher than the former values by 0.27 ± 0.18 and E_A lower by 1.21 ± 0.42 kcal·mol^{-1}. According to MM3 calculations[24−26] the standard heat of formation ($\Delta H_f°$) of **12** is 32.01 kcal·mol^{-1}. Together with the E_A value of 46.07 ± 1.18 kcal·mol^{-1}, this adds up to 78.08 ± 1.18 kcal·mol^{-1} for the $\Delta H_f°$ of the transition state for **12** ⇄ **13**.

For comparison, $\Delta H_f°$ of the transition state for **15** ⇄ **12** was estimated.

The calculation of $\Delta H_f°$ of the diradical **15** makes use of the observation that the two C_8 rings of *l*-bicyclooctyl-2,2′-diene-4,4′-dione (**30**, Scheme 12), according to MM3-VESCF calculations,[24−26] retain excellent coplanarity of their enone π-systems irrespective of the angle of rotation about the central bond connecting the two C_8 rings. This means that **30** is an excellent steric model for **15**, the allyl π-systems of which should similarly retain coplanarity irrespective of the angle of rotation. The $\Delta H_f°$ of **15** was therefore computed from the $\Delta H_f°$ values of **30**, of methyl vinyl ketone (both by MM3-VESCF) and of 1-methylallyl radical[22] by subtraction and addition. From $\Delta H_f°$ of the *anti* conformer of **30** (−52.97 kcal·mol^{-1}), $\Delta H_f°$ of **15*a*** (Scheme 4) was determined as 66.6 kcal·mol^{-1}, whereas from $\Delta H_f°$ of one *gauche* conformer of **30** (−54.54 kcal·mol^{-1}), the $\Delta H_f°$ of **15*g*12** (Scheme 4) was determined as 65.1 kcal·mol^{-1}. Together with the height of the barrier separating **15** from **12** as obtained from the oxygen experiments (10.2 ± 1.5 kcal·mol^{-1}), this yields 76.8 ± 1.5 kcal·mol^{-1} for $\Delta H_f°$ of the barrier separating **15** from **12** if ring-closure to **12** started from **15*a***, and 75.3 ± 1.5 kcal·mol^{-1} if it started from **15*g*12**. These two values are quite similar to the $\Delta H_f°$ value obtained for the transition state for **12** ⇄ **13** (78.08 ± 1.18 kcal·mol^{-1}).

According to the above reasoning, the relative $\Delta H_f°$ values of the rotamers about the central bond of **15** should be the same as for **30**. The latter were computed by MM3-VESCF. Accordingly, we obtained relative $\Delta H_f°$ values for **15*g*12** (Scheme 4) ≡ 0, for **15*gg*** = 10.76, for **15*g*13** = 0.55, for **15*ag*13** = 12.68, for **15*a*** = 1.57 and for **15*ag*12** = 9.28 kcal·mol^{-1}. Analogously, for the case of **14**, we obtained relative $\Delta H_f°$ values for **14*a*** ≡ 0, for **14*ag*** = 10.5, for **14*g*** = 2.37 and for the barrier separating the two enantiomers of **14*g*** = 15.07 kcal·mol^{-1}. The main cause of the unexpectedly high rotational barriers emerging from these values appears to be the stiffness of the C_8 rings; the rings won't budge when passing each other on top of the rotational barrier. These high calculated rotational barriers might well

Table 5. Kinetics of thermolysis of **12** (→ **13** + **16**) and of **13** (→ **12** + **16**) in the gas phase (16 hPa, no added gases, conversions below 7 %)

T [°C]	220	230	240	250	260
12 → **13** + **16**					
$10^8\ k_{\mathbf{12}\rightarrow\mathbf{13}} \times$ s	1.74 ± 0.14	4.68 ± 0.28	10.57 ± 0.51	24.60.± 1.80	61.61.± 3.47
[**16**]/[**13**]	6.31 ± 0.20	6.30 ± 0.25	6.02 ± 0.04	5.91 ± 0.08	5.77 ± 0.11
13 → **12** + **16**					
$10^8\ k_{\mathbf{13}\rightarrow\mathbf{12}} \times$ s				62.5 ± 1.5	
[**16**]/[**12**]				0.73 ± 0.03	

represent the high barriers protecting **14** and **15**, if one allows for the limited accuracy of MM3-derived barrier heights in regimes of rather high barriers.[66]

The following conclusions emerge. The thermal interconversion between **12** and **13** must necessarily involve both *gauche* diradicals **15*g*12** and **15*g*13**; a priori, it may or may not also involve **15*a*** (Scheme 4). Structure **16**, which is also formed in the course of this interconversion, must arise by ring-closure of **15*g*12** or **15*g*13** or both. The fact that **12** and **13**, when formed from **9**, are virtually unaccompanied by **16** ([**12**]/[**16**] ≈ 200; [**13**]/[**16**] ≈ 43; vide supra) even though they must be formed by ring-closure of **15*g*12** and **15*g*13**, respectively, implies that in the course of the interconversion **12** ⇄ **13, 16** must arise by ring-closure of **15*g*12** when formed from **12** in amounts similar to **13**, and must arise by ring-closure of **15*g*13** when formed from **13** in amounts similar to **12**. These facts furthermore imply that the rate-determining barrier for the interconversion **12** ⇄ **13** (78.08 ± 1.18 kcal·mol^{-1}) must be one of the rotational barriers, either **15*gg*** or **15*ag*12**/**15*ag*13** (Scheme 4). These were estimated above by MM3 calculations as 75.86 and 77.78 kcal·mol^{-1}, respectively, which would therefore suggest **15*gg*** as the rate-determining barrier. The discrepancy between the two values, 75.86 and 78.08 ± 1.18 kcal·mol^{-1}, is within the limits of the accuracy of the MM3 plus group-increment methods.

Dimerisation of 9 in the Presence of Spin = 1/2 Transition Metal Complexes

Bis[2-(2-ethylhexyl)cyclohexane-1,1′-dionato]copper(II) (**Cu**) is a highly alkylated derivative of the spin = 1/2 metal complex bis(acetylacetonato)copper(II); it is highly soluble in *n*-octane due to its extensive alkylation. The presence of high concentrations of **Cu** in *n*-octane did not influence the rates of formation of dimer **11** and of the sum of dimers **12** + **13**, and thus did not influence the ratio [**11**]/[**12** + **13**]; these values were the same as they were without **Cu** under argon. There was one spectacular change, however; the ratio [**12**]/[**13**] at 25 °C increased from 4.59 in *n*-octane under argon in the absence of **Cu** to up to 12.5 in the presence of 0.24 M **Cu**. That is, **Cu** increased the amount of **12** that was formed, at the expense of the amount of **13** that was formed. Since the rates of formation of total **13** in the presence of high concentrations of **Cu** approached the rate of formation of untrappable **13** (Table 4), it is obvious that **Cu** affected only the trappable but not the untrappable **13**. In terms of trappable **12** and **13** only, **Cu** increased the ratio $R \equiv (k_{\mathbf{12}} - {}_{\mathrm{U}}k_{\mathbf{12}})/(k_{\mathbf{13}} - {}_{\mathrm{U}}k_{\mathbf{13}})$ from $R_0 = ({}_0k_{\mathbf{12}} - {}_{\mathrm{U}}k_{\mathbf{12}})/({}_0k_{\mathbf{13}} - {}_{\mathrm{U}}k_{\mathbf{13}}) = 6.49 \pm 0.23$ observed in the absence of **Cu** to values of ca. 40 observed with 0.24 M **Cu**, where ${}_{\mathrm{U}}k_{\mathbf{12}}$ is the rate of formation of untrappable **12**, ${}_0k_{\mathbf{12}}$ is the rate of formation of total **12** in the absence of **Cu**, and $k_{\mathbf{12}}$ is the rate of formation of total **12** in the presence of a given [**Cu**], an analogous situation holding for **13** (all in *n*-octane under argon, 25 °C). The obvious explanation for these phenomena is that **15**, created in its singlet spin state, is converted into triplet-state **15** on encounter with the unpaired spin of **Cu**, and that the two spin states of **15** form **12** and **13** in quite different proportions. The situation can be described by the general reaction scheme shown in Scheme 7 (which excludes untrappable **12** and untrappable **13**), where **C** is a spin-active catalyst such as **Cu**, S-**15** and T-**15** are the singlet and triplet spin states, respectively, of **15**, and $\mathbf{A}_l$ is a trapping product of **15** by **C** (there is none if **C** = **Cu**). By use of the quasi-steady-state conditions for S-**15** and T-**15**, the reaction scheme translates into the equations shown in Scheme 7. The linear Equation (1) relates the experimentally determined variables $(R - R_0)^{-1}$ [Equation (2)] and $[\mathbf{Cu}]^{-1}$ to the constant parameters *B* and *C*. To determine *B* and *C* at 25 °C, dimerisations of **9** were carried out at six concentrations of [**Cu**] in the range 0.0232−0.243 M, and the resulting ratios [**12**]/[**13**] were determined. To make sure that **Cu** did not form aggregates in *n*-octane, dimerisations were also carried out in the presence of varying amounts of tetrahydrofuran (THF), which would suffice to break up any aggregates (molar ratio THF/**Cu** > 2); both the rates of dimerisation and the ratios [**12**]/[**13**] were independent of added THF, however. A plot according to Equation (1) exhibited the expected linearity (Figure 5) and afforded the values for *B* and *C* presented in Figure 5. Quantity *B* represents $(R - R_0)^{-1}$, as would be found at [**Cu**] = ∞. The value obtained for *B* (0.0102 ± 0.0034) thus translates into a value of 80−150 for R_∞; that is, for $(k_{\mathbf{12}} - {}_{\mathrm{U}}k_{\mathbf{12}})/(k_{\mathbf{13}} - {}_{\mathrm{U}}k_{\mathbf{13}})$ as would be found experimentally under conditions of perfect equilibrium between S-**15** and T-**15** (i.e., at [**Cu**] = ∞). As can be derived from the analytic expression for *B* [Equations (3) and (5), Scheme 7], ${}_{\mathrm{T}}k_{\mathbf{12}}/{}_{\mathrm{T}}k_{\mathbf{13}}$ must amount to at least this value for R_∞. The complicated expression for

the quantity C [Equations (4) to (6), Scheme 7] can be greatly simplified to a good approximation: $A \approx 1$ (since ${}_{S}k_{12}/{}_{S}k_{13} = 6.49$ whereas ${}_{T}k_{12}/{}_{T}k_{13} \geq 80$, vide supra) and $(1 + {}_{T}k_{13}/{}_{T}k_{12}) \approx 1$ (since ${}_{T}k_{12}/{}_{T}k_{13} \geq 80$, vide supra). The expression for C thus reduces to ${}_{S}k_{13}/{}_{S}k_{T}$ (i.e., the ratio of the rate constants for two competing reactions of S-**15**, unimolecular ring-closure to form **13** and bimolecular conversion into T-**15** by **Cu**). Together with the values for ${}_{S}k_{12}/{}_{S}k_{13}$ ($= 6.49 \pm 0.23$) and ${}_{S}k_{12}$ [$\equiv {}_{12}k_{RC} = (16.31 \pm 0.78) \times 10^5$ s^{-1}, Table 4, Column 8], the value obtained for C (0.00551 ± 0.00017 M) thus yields ${}_{S}k_{T} = (4.56 \pm 0.31) \times 10^7$ s^{-1} M^{-1} for the rate constant for bimolecular conversion of S-**15** to T-**15** by **Cu** at 25 °C. By another line of reasoning, we can write: $R = ([\text{S-}\mathbf{15}]\,{}_{S}k_{12} + [\text{T-}\mathbf{15}]\,{}_{T}k_{12})/([\text{S-}\mathbf{15}]\,{}_{S}k_{13} + [\text{T-}\mathbf{15}]\,{}_{T}k_{13})$, where [S-**15**] and [T-**15**] are steady-state concentrations in the presence of a given [**Cu**]. The equation rearranges to $R(1 + G\,{}_{T}k_{13}/{}_{S}k_{13}) = ({}_{S}k_{12} + G\,{}_{T}k_{12})/{}_{S}k_{13}$, where $G \equiv$ [T-**15**]/[S-**15**]. Hence, $R < ({}_{S}k_{12} + G\,{}_{T}k_{12})/{}_{S}k_{13}$, which rearranges to $F \equiv G\,{}_{T}k_{12}/{}_{S}k_{12} > (R\,{}_{S}k_{13}/{}_{S}k_{12} - 1) = (R/R_0 - 1)$. Quantity F represents the ratio of **12** formed through the triplet over **12** formed through the singlet state. For [**Cu**] = 0.243 M, from R_0 and the pertinent R value, F is found to be > 5; for perfect equilibrium between S-**15** and T-**15**, from R_0 and R_∞, F_∞ is found to be > 11. The value $RT\ln F_\infty$ represents the free-energy difference between the two rate-determining transition states, denoted by S-**15***TS***12** and T-**15***TS***12**, affording **12** from S-**15** and from T-**15**, respectively. T-**15***TS***12** is thus found to be lower in free energy of formation than S-**15***TS***12** by > 1.4 kcal·mol^{-1}. T-**15***TS***13**, in contrast, must be much less lower than S-**15***TS***13**; the free energy difference S-**15***TS***12** − T-**15***TS***12** − S-**15***TS***13** + T-**15***TS***13** amounts to $\geq RT\ln R_\infty/R_0$ (bearing in mind that ${}_{T}k_{12}/{}_{T}k_{13} \geq R_\infty$), that is, ≥ 1.5 kcal·mol^{-1}.

Cobaltocene, $(C_5H_5)_2Co$ (**Co**), is another spin = 1/2 transition metal complex highly soluble in *n*-octane. It was found to be more efficient than **Cu**, producing the same effects as **Cu** but requiring considerably lower concentrations. It had two technical drawbacks, however, with respect to **Cu**. Firstly, **Co** in solution is extremely sensitive towards atmospheric oxygen, which rapidly oxidises it to the spin = 0 cation $\mathbf{Co}^+$; in spite of all precautions taken, meaningful R values could not be obtained with very dilute solutions of **Co**. Secondly, **Co** noticeably trapped **14** and **15** to give adducts **A** (Scheme 7),[67] which were not isolated; with [**Co**] = 0.1 M, values for k_{12} and k_{13} were reduced to ca. two thirds of what they were in the absence of **Co**. Meaningful R values were determined with [**Co**] = 0.029−0.1 M. {At lower [**Co**] values, the $(R - R_0)^{-1}$ values were poorly reproducible and on average too high for the reasons mentioned, causing a strong upwards curvature of the expected linear plots. At higher [**Co**] values, $(k_{13} - {}_{U}k_{13})$ became too small a difference between two large numbers for significant values to be obtained.} A linear regression analogous to **Cu** produced $B = 0.0086 \pm 0.0019$ and $C = (0.000269 \pm 0.000083)$ M. Within the error limits, B is the same for **Co** and **Cu** [the expressions for B (Scheme 7) are the same for **Cu** as for **Co** except for ${}_{T}k_{A}$]; C, however, is quite different from what it was in the case of **Cu** and in analogy to the above yields ${}_{S}k_{T} = (9.3 \pm 2.9) \times 10^8$ s^{-1} M^{-1} for the rate constant for bimolecular conversion of S-**15** to T-**15** by **Co** (*n*-octane, 25 °C).

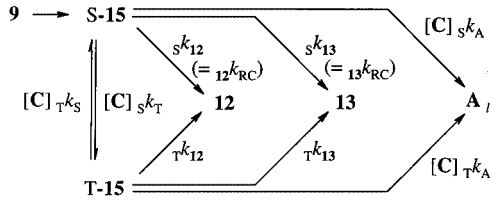

$$(R - R_0)^{-1} = B + C\,[\mathbf{C}]^{-1} \qquad (1)$$

$$R - R_0 \equiv \frac{k_{12} - {}_{U}k_{12}}{k_{13} - {}_{U}k_{13}} - \frac{{}_{0}k_{12} - {}_{U}k_{12}}{{}_{0}k_{13} - {}_{U}k_{13}} \qquad (2)$$

$$B = \left[\frac{({}_{T}k_{S} + {}_{T}k_{A})\,{}_{S}k_{13}}{{}_{T}k_{12}\,{}_{S}k_{T}} + \frac{{}_{T}k_{13}}{{}_{T}k_{12}}\right]A^{-1} \qquad (3)$$

$$C = [(1 + {}_{T}k_{13}/{}_{T}k_{12})\,{}_{S}k_{13}/{}_{S}k_{T}]\,A^{-1} \qquad (4)$$

$$A = 1 - \frac{{}_{S}k_{12}\,{}_{T}k_{13}}{{}_{S}k_{13}\,{}_{T}k_{12}} \qquad (5)$$

$${}_{S}k_{12}/{}_{S}k_{13} = \frac{{}_{0}k_{12} - {}_{U}k_{12}}{{}_{0}k_{13} - {}_{U}k_{13}} \qquad (6)$$

$$\frac{[\mathbf{A}_l]}{[\mathbf{12} + \mathbf{13}][\mathbf{C}]} = \frac{{}_{S}k_{A}[D + {}_{T}k_{A}/({}_{T}k_{12} + {}_{T}k_{13})]}{({}_{S}k_{12} + {}_{S}k_{13})[D + {}_{S}k_{A}/({}_{S}k_{12} + {}_{S}k_{13})]} \qquad (7)$$

$$D = \{[\mathbf{C}]^{-1} + ({}_{T}k_{S} + {}_{T}k_{A})/({}_{T}k_{12} + {}_{T}k_{13})\}\,{}_{S}k_{A}/{}_{S}k_{T} \qquad (8)$$

Scheme 7. Kinetic scheme for the reactions involving the "trappable" diradicals **15** in their singlet (S-**15**) and triplet (T-**15**) spin states; the "untrappable" diradicals **15** are not considered in this scheme; **C** is a spin inversion catalyst for **15** that in addition may or may not form adducts $\mathbf{A}_l$ with **15**; an analogous scheme holds for trappable **14**

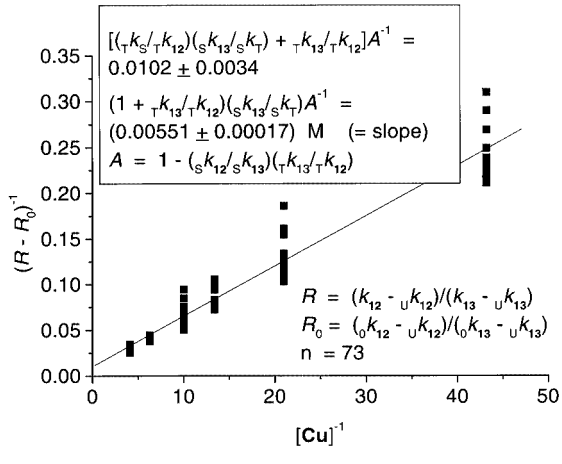

Figure 5. Plot of the dependence of the ratio of "trappable" **12** over "trappable" **13** (*n*-octane, 25 °C) on the concentration of bis[2-(2-ethylhexyl)cyclohexane-1,1′-dionato]copper(II) (**Cu**)

Xenon is known to be an efficient singlet-to-triplet spin conversion catalyst, due to a heavy-atom effect.[68] Dimerisation of **9** at ambient conditions under xenon in place of argon, however, revealed no effect; nor did 1.7 M tetrabromomethane produce an effect.

The following conclusions emerge:

i. S-**15** (singlet spin state) is converted into T-**15** (triplet spin state) by **Co** and **Cu** with bimolecular rate constants of $(9.3 \pm 2.9)\times10^8$ and $(4.56 \pm 0.31)\times10^7$ s^{-1} M^{-1}, respectively (*n*-octane, 25 °C). The dimer ratios **12/13** (excluding untrappable **12** and **13**) formed from S-**15** and T-**15** differ dramatically: 6.49 ± 0.23 for S-**15** but ≥ (80−150) for T-**15**. At 0.243 M **Cu**, more than 80% of trappable dimers **12** and **13** arise from T-**15**. The rate-determining barrier for the reaction T-**15** → **12** is lower in free energy of formation than the rate-determining barrier for the reaction S-**15** → **12** by > 1.4 kcal·mol^{-1}; for **13**, in contrast, the triplet barrier is relatively higher than the singlet barrier by ≥ 1.5 kcal·mol^{-1}, as compared to the former case. Nothing can be said about the position of the equilibrium [T-**15**]/[S-**15**], though.

ii. In the presence of dioxygen (but in the absence of **Cu** and **Co**), the dimer ratio **12/13** (excluding untrappable **12** and **13**) was unchanged with respect to its value in the absence of dioxygen and of other agents (vide supra). Hence, dioxygen, though existing in a triplet spin state, did not change the spin state of **15** that was not irreversibly trapped by it.

iii. The fact that the dimer ratio **12/13** can be shifted by spin-active agents implies that both **12** and **13** arise from the same S-**15** species (considering only trappable **12** and **13**). Since in the preceding section the conclusion was reached that the barrier separating the two *gauche* diradicals S-**15*g*12** and S-**15*g*13** (by whatever reaction path) must be higher than the barriers separating S-**15*g*12** from **12** and S-**15*g*13** from **13**, this is only possible if S-**15** is created as S-**15*a*** (Scheme 4); furthermore, the rotational barriers S-**15*ag*12** and S-**15*ag*13** must be the rate-determining barriers (called S-**15***TS***12** and S-**15***TS***13** above) between S-**15*a*** and **12** and **13**, respectively. The MM3-derived value for S-**15*ag*12**, of 7.71 kcal·mol^{-1} relative to S-**15*a*** (vide supra), is significantly lower than the experimental value of 10.21 ± 1.5 kcal·mol^{-1}, which, however, is within the limits of accuracy of the methods.

iv. The sum of the rate constants for formation of trappable **12** and trappable **13** from **9** equals the rate constant for formation of S-**15*a*** from **9**. The Arrhenius plot for this sum is displayed in Figure 6.

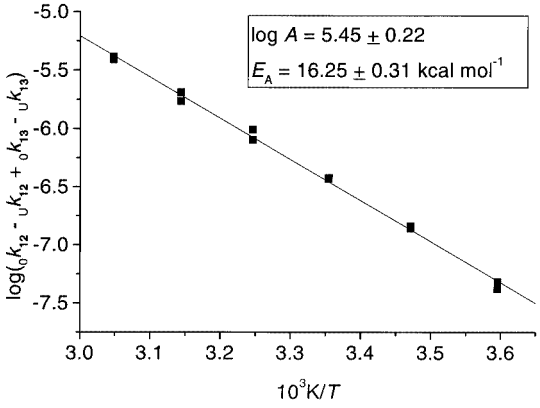

Figure 6. Arrhenius plot of the bimolecular rate constants for the formation of the sum of "trappable" dimer **12** and of "trappable" dimer **13** from **9** in *n*-octane

Dimerisation of 9 in the Presence of Nitroxyls ($R_2NO\cdot$), Part 2

Since it is a spin = 1/2 species that traps carbon-centred radicals at rates well below diffusion control in *n*-octane at 25 °C,[45−47] nitroxyl **17** should be expected to influence the **12/13** ratio similarly to **Cu** and **Co**. This was found to be the case. Observed *R* values (*n*-octane, 25 °C) ranged from 10 ([**17**] = 0.0038 M) to 29−33 ([**17**] = 0.105 M), yielding $B = 0.020 \pm 0.0042$ and $C = (8.46 \pm 0.70)\times10^{-4}$ M [Equation (1), Scheme 7]. The *C* value translates (vide supra) into an $_Sk_T$ value of $(2.97 \pm 0.30)\times10^8$ s^{-1} M^{-1} for the bimolecular conversion of S-**15*a*** to T-**15*a*** by **17**. From the same set of experiments, values for the ratio $[\mathbf{A}_l]/([\mathbf{12}+\mathbf{13}]\times[\mathbf{17}])$, where $\mathbf{A}_l$ (Scheme 7) denotes *l*-(2:2) trapping products by **17**, as well as for the analogous ratio $[\mathbf{A}_u]/([\mathbf{11}]\times[\mathbf{17}])$ (trappable **11**, **12** and **13** only) depending on [**17**] were obtained and are presented in Table 6. The values turned out to be constant within the error limits in the observed range of [**17**] (= 0.0038−0.105 M), as would be expected if one single species each of **14** and **15**, either S or T, were operative throughout the range. However, as documented by the *R* values, there is a change from predominantly S-**15** at [**17**] = 0.0038 M to predominantly T-**15** at [**17**] = 0.105 M. As follows from Equation (7) in Scheme 7, for such constancy to be observed, any one of three conditions (1) to (3) must be fulfilled to a sufficiently good approximation over the entire range of [**17**] (0.0038−0.105 M): (1) $[\mathbf{17}]^{-1} >> (L+M)$ and $[\mathbf{17}]^{-1} >> (L+N)$, where $L = ({}_Tk_S + {}_Tk_\mathbf{A})/({}_Tk_\mathbf{12} + {}_Tk_\mathbf{13})$, $M = ({}_Sk_T/{}_Sk_\mathbf{A})\times{}_Tk_\mathbf{A}/({}_Tk_\mathbf{12} + {}_Tk_\mathbf{13})$ and $N = {}_Sk_T/({}_Sk_\mathbf{12} + {}_Sk_\mathbf{13})$; (2) $[\mathbf{17}]^{-1} << (L+M)$ and $[\mathbf{17}]^{-1} << (L+N)$; (3) ${}_Tk_\mathbf{A}/({}_Tk_\mathbf{12} + {}_Tk_\mathbf{13}) \approx {}_Sk_\mathbf{A}/({}_Sk_\mathbf{12} + {}_Sk_\mathbf{13})$. An analogous situation exists for $\mathbf{A}_u$ and **11** in place of $\mathbf{A}_l$ and **12** + **13**, as follows from Equation (7) after carrying out the proper substitutions. By using Equation (3) in Scheme 7 and bearing in mind $A \approx 1$, $C \approx {}_Sk_\mathbf{13}/{}_Sk_T$, and ${}_Tk_\mathbf{13} << {}_Tk_\mathbf{12}$ (vide supra), one obtains $L \approx (B - {}_Tk_\mathbf{13}/{}_Tk_\mathbf{12})/C$ and $N \approx [C\times(1 + {}_Sk_\mathbf{12}/{}_Sk_\mathbf{13}]^{-1}$. Insertion of the proper values (vide supra) yields $(L+N) = 174 \pm 19$ M^{-1}. Since $[\mathbf{17}]^{-1}$ ranges from 9.5 to 263 M^{-1}, it is clear that condition (1) is fulfilled only for the lowest [**17**] applied (0.0038 M), but not for the other ones, which range from 0.0057 to 0.105 M. Condition (1) can thus be dismissed as a possibility, but condition (2), being the reverse of (1), cannot. Condition (1) would have represented the limiting case when [**17**] was so low that virtually pure S-**15** was operative. Condition (3) would simplify Equation (7) to $[\mathbf{A}_l]/([\mathbf{12}+\mathbf{13}]\times[\mathbf{17}]) = {}_Sk_\mathbf{A}/({}_Sk_\mathbf{12} + {}_Sk_\mathbf{13})$; analogously, $[\mathbf{A}_u]/([\mathbf{11}]\times[\mathbf{17}]) = {}_Sk_\mathbf{A}/{}_Sk_\mathbf{11}$. With the values in Table 6 and with the known values for ${}_Sk_\mathbf{11}$, ${}_Sk_\mathbf{12}$ and ${}_Sk_\mathbf{13}$ (denoted as ${}_{11}k_{RC}$, ${}_{12}k_{RC}$ and ${}_{13}k_{RC}$ in Table 4), these equations yield ${}_Sk_\mathbf{A}$ values of $(3.02 \pm 1.03)\times10^7$

s^{-1} M^{-1} and $(3.44 \pm 1.13)\times10^7$ s^{-1} M^{-1} for the trapping of diradicals S-**14** and S-**15**, respectively, by **17**. These values are significantly lower than those reported for trapping of comparable carbon-centred monoradicals with **17** (4.6×10^8, 1.9×10^8 and 6.2×10^7 s^{-1} M^{-1} for benzyl, α-methylbenzyl and α,α-dimethylbenzyl, respectively[47]) even though S-**14** and S-**15** have two equivalent sites of attack whereas the three monoradicals have only one. Evidence that these values for ${}_Sk_A$ are indeed too low is given below, and rules out condition (3). What remains is condition (2), with the added requirement ${}_Tk_A/({}_Tk_{12} + {}_Tk_{13}) << {}_Sk_A/({}_Sk_{12} + {}_Sk_{13})$ in order to raise ${}_Sk_A$ to appropriate values.

Table 6. Ratio of trapping products (A_u and A_l) of **14** and **15**, respectively, by **17**, over dimers **11** and (**12** + **13**) ("trappable" dimers only), respectively, divided by [**17**], in dependence on [**17**] (*n*-octane, 25°C)

[**17**]/M	$[A_u]\times M/([11][17])$	$[A_l]\times M/([12+13][17])$	*n*
0.0038	18.16 ± 2.44	20.94 ± 3.02	2
0.0057	14.64	17.27	1
0.0120	11.58 ± 2.86	14.39 ± 3.75	3
0.0235	14.62 ± 3.20	17.71 ± 3.94	6
0.036	16.34 ± 1.11	19.08 ± 1.41	5
0.062	15.81 ± 0.32	18.10 ± 0.37	4
0.105	17.69 ± 1.39	20.30 ± 1.95	6
0.0038−0.105	15.46 ± 3.38	18.25 ± 3.66	27
0.19	20.53 ± 0.58	23.51 ± 0.76	6
0.37	23.06 ± 0.66	25.94 ± 1.17	6
0.57	24.73 ± 1.95	27.56 ± 1.37	13
1.1	29.14 ± 3.26	35.95 ± 3.41	13
2.3	34.55 ± 3.38		10

Whichever condition, (2) or (3) [(1) being safely dismissed], is fulfilled, they both agree that the observed constancy of $[A_l]/([12+13]\times[17])$ and $[A_u]/([11]\times[17])$ should continue on proceeding to ever higher [**17**]. This, however, was not the case. When the range of [**17**] was extended up to 2.3 M, a significant increase in the values for $[A_l]/([12+13]\times[17])$ and $[A_u]/([11]\times[17])$ was observed (Table 6, lower part); this increase was not noticeable in the absolutely (though not relatively) very much narrower range of 0.0038−0.105 M. A plot of $[A_u]/([11]\times[17])$ vs. [**17**] is curved and appears to approach a limiting value of 40−45 at infinite [**17**]. One conceivable explanation for the phenomenon might be a reversible addition of the first molecule of **17** to **14** or **15** followed by irreversible addition of the second molecule of **17**, thus causing a kinetic order higher than 1 with respect to **17**, approaching 2. However, this higher order should appear more pronounced for lower [**17**], which is at variance with the reaction order of 1 found in the range of the lowest [**17**], which expresses itself in the constancy of $[A_l]/([12+13]\times[17])$ and $[A_u]/([11]\times[17])$ in this range. Further evidence that the irreversible trapping of **14** and **15** is kinetically of first order with respect to **17** is given below. This explanation being dismissed, the only explanation that appears to remain is that diradicals **14** and **15**, after having been exposed to the chance of being trapped by **17** and having survived by crossing the rate-determining barrier to ring-closure, again find themselves in a state in which they cannot ring-close immediately, but are exposed to the chance of being trapped by **17** for a second time before they can finally close the ring. Since this second state can only be another form of diradicals **14** and **15**, this means that **14** and **15** are generated as ***14a*** and ***15a***, which are first converted in the rate-determining step to ***14g*** and ***15g***, which then ring-close. In the presence of more than 0.1 M of **17**, most ***14a*** and ***15a*** will cross the rate-determining barrier in their triplet spin states (vide supra); the triplet ***14g*** and ***15g*** thus generated cannot ring-close immediately but have to await spin inversion, and during this lifetime they can be trapped by **17**. The fact that $[A_l]/([12+13]\times[17])$ and $[A_u]/([11]\times[17])$ do not increase linearly with [**17**], but rather approach a limiting value as indicated above, suggests that triplet ***14g*** and ***15g*** can undergo two competing reactions on encounter with **17**: trapping and induced spin inversion to singlet ***14g*** and ***15g***, which then ring-close immediately. Scheme 8 shows the pertinent reaction scheme and the equation derived from it. By this equation, it is possible to obtain rough estimates of ${}_Tk'_A/{}_Tk'_S = 1.9$, ${}_Tk'_A/{}_Tk'_{11} = 1.8$ M^{-1} and ${}_Tk_A/{}_Tk_{11} = 13.7$ M^{-1} from the limiting values for $[A_u]/([11]\times[17])$ at zero and at infinite [**17**] and from the slope at zero [**17**]. A similar treatment can be applied to the *l* case and results in similar values. Scheme 8 reveals that Scheme 7 in its triplet part is actually an oversimplification; at zero [**17**], $[A_u]/([11]\times[17])$ should equal ${}_Tk_A/{}_Tk_{11} + {}_Tk'_A/{}_Tk'_{11}$ rather than ${}_Tk_A/{}_Tk_{11}$ as suggested in Scheme 7. In view of the values (${}_Tk'_A/{}_Tk'_{11} = 1.8$ M^{-1} and ${}_Tk_A/{}_Tk_{11} = 13.7$ M^{-1}), however, the error committed is moderate.

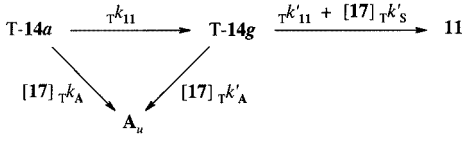

$$\frac{[A_u]}{[11][17]} = \frac{{}_Tk'_A(1 + [17]\,{}_Tk_A/{}_Tk_{11})}{{}_Tk'_{11}(1 + [17]\,{}_Tk'_S/{}_Tk'_{11})}$$

Scheme 8

When paraffin oil (η = 85.7 cP at 25 °C; purified so as to contain saturated hydrocarbons only) was used in place of *n*-octane, dimer ratios and dimerisation rate constants in the absence of additives were similar to those observed in *n*-octane. The results obtained in the presence of **17**, however, were characteristically different from those observed in *n*-octane and are shown in Table 7 for the *u* case; the result for the *l* case is analogous. In contrast to *n*-octane, in which $[A_u]/([11]\times[17])$ was approximately constant between [**17**] = 0.0038 M and 0.1 M but increased on going from

[**17**] = 0.1 to 2.3 M, [$\mathbf{A}_u$]/([**11**]×[**17**]) was now constant within the error limits throughout the observed range of [**17**] from 0.01 to 0.48 M. The reason was that, because of the high viscosity of the medium, the trapping of **14** by **17** was diffusion-controlled in paraffin oil. This means that any encounter of **14** with **17** should result in irreversible trapping and consequently, that no T-**14*a*** escaping from the encounter with **17** will be generated; consequently, no T-**14*g*** will be formed by crossing the ***a***-to-***g*** barrier, but only S-**14*g***, which will immediately ring-close to **11** and will not be trapped by **17**. Therefore, [$\mathbf{A}_u$]/([**11**]×[**17**]) = ${}_{S}k_{\mathbf{A}}/{}_{\mathbf{11}}k_{RC}$, where ${}_{S}k_{\mathbf{A}}$ is the rate constant for diffusion-controlled bimolecular trapping of S-**14** and ${}_{\mathbf{11}}k_{RC}$ is assumed to have the same value as in *n*-octane: (1.95 ± 0.11)×10^6 s^{-1}. From this and from the observed mean value for [$\mathbf{A}_u$]/([**11**]×[**17**]), of 28.1 ± 9.1 M^{-1}, one obtains ${}_{S}k_{\mathbf{A}}$ = (5.5 ± 1.8)×10^7 s^{-1} M^{-1}, which compares well with the value predicted from the Stokes−Einstein equation, 7.7×10^7 s^{-1} M^{-1}. The following conclusions emerge. Firstly, on one hand the value ${}_{S}k_{\mathbf{A}}$ = (5.5 ± 1.8)×10^7 s^{-1} M^{-1} is higher than the value ${}_{S}k_{\mathbf{A}}$ = (3 ± 1)×10^7 s^{-1} M^{-1} obtained above for the absence of diffusion control on the basis of condition (3). This, however, is impossible since, on the contrary, the value obtained in the absence of diffusion control must be higher than the one obtained under diffusion control. This rules out condition (3), as mentioned above. On the other hand, a value for ${}_{S}k_{\mathbf{A}}$ in the absence of diffusion control of (3.8 ± 0.4)×10^8 s^{-1} M^{-1}, estimated from the literature value for α-methylbenzyl after inclusion of a statistical factor of 2,[47] is consistent with the value obtained under diffusion control. It is still not very much larger than the latter, which means that the trapping reaction should already be out of diffusion control if the viscosity of the medium is even as much as one tenth of that of the paraffin oil used. Indeed, in *n*-hexadecane (η = 3.3 cP) as solvent, the trapping behaviour matched that observed in *n*-octane rather than that observed in paraffin oil. Secondly, the constancy of [$\mathbf{A}_u$]/([**11**]×[**17**]) under diffusion control means that the irreversible trapping of **14** is a reaction that is kinetically first order with respect to **17**, in confirmation of a conclusion arrived at above.

The following conclusions emerge from this section. Firstly, nitroxyls catalyse singlet-to-triplet spin inversion of diradicals **14*a*** and **15*a*** similarly to spin = 1/2 transition metal complexes. The rate constant of (2.97 ± 0.30)×10^8 s^{-1} M^{-1} for the S-**15*a*** to T-**15*a*** conversion by **17** happens to be similar to the rate constant, estimated from literature values, for competing trapping by **17**. The trapping of S-**14*a*** and S-**15*a*** is kinetically first order with respect to **17**. Secondly, it was demonstrated in the previous section that S-**15** is generated as S-**15*a***. This section independently demonstrates that S-**14** and S-**15** are generated as S-**14*a*** and S-**15*a***, respectively. This follows from the kinetics of trapping by **17**, which show that T-**14** and T-**15** are twice exposed to the chance of being trapped, first in their ***a*** and then in their ***g*** conformations.

Table 7. Ratio of trapping product $\mathbf{A}_u$ of **14** by **17**, over dimer **11** ("trappable" **11** only), divided by [**17**], in dependence on [**17**] (paraffin oil, η = 85.7 cP, 25°C)

[**17**]/M	[$\mathbf{A}_u$]×M/([**11**][**17**])	*n*
0.010	30.1 ± 4.2	4
0.020	28.5 ± 2.9	5
0.029	28.9 ± 3.7	3
0.061	27.1 ± 6.8	3
0.089	27.5 ± 3.6	2
0.116	24.7 ± 0.8	3
0.297	28.2 ± 3.2	6
0.480	28.3 ± 7.4	2
	28.1 ± 9.1	28

The Mechanism of Dimerisation of 9

From the above, the mechanism of the thermal dimerisation of **9** emerges as follows. In the rate-determining step, two molecules of **9** combine irreversibly to form the *anti* 1,4-diradicals **14*a*** and **15*a*** in their singlet-spin states. Singlet **14*a*** and **15*a*** are stable species of rather long lifetimes (ca. 0.5 μs), and are protected by energy barriers of 11.1 ± 1.5 and 10.2 ± 1.5 kcal·mol^{-1}, respectively. After crossing these barriers to form the *gauche* 1,4-diradicals **14*g*** and **15*g***, these ring-close to form the final dimers **11** and **12** + **13**, respectively. Thus, the dimerisation of **9** occurs in two strictly separated steps, the first new C−C single bond being formed in the first step and the second new C−C single bond being formed in the second step. The corresponding reaction diagram featuring heats of formation (kcal·mol^{-1}) obtained from the literature or elaborated in the current work is shown in Scheme 9. One value in parentheses represents the heat of formation of the transition state for the interconversion **12** ⇄ **13**; this transition state may be identical to **15*ag*12** or **15*ag*13** if the interconversion involves **15*a***. The energetics presented in Scheme 9 contrast strikingly with those for the parent system, butadiene and its dimers, presented in Scheme 2. Firstly, 2 × **9** is higher in energy than the 1,4-diradicals, which is due to the high strain of **9**.[16] Secondly, the barriers separating **9** from **14*a*** and **15*a*** are very much higher than the analogous barriers in the butadiene parent system. The reason for this are geometric constraints at the top of the barriers, which prevent the π orbitals on C-2 and C-2′ from achieving good overlap with those on C-1 and C-1′ (which form the central C−C bond connecting both rings) and also prevent them from achieving good overlap (and hence from achieving allylic stabilisation) with those on C-3 and C-3′. The same is true for the analogous barriers separating **14*a*** and **15*a*** from (*Z,Z*)-cycloocta-1,3-diene. Thirdly, the rotational barriers **14*ag***, **15*ag*12** and **15*ag*13** are also extraordinarily high as compared to the parent butadiene system. The main reason for this appears to be the stiffness of the allylic C_8 rings, which won't budge when passing each other on top of the rotational barriers.

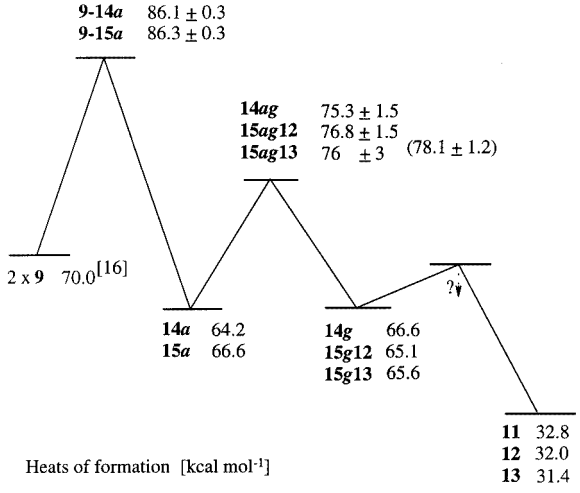

Scheme 9

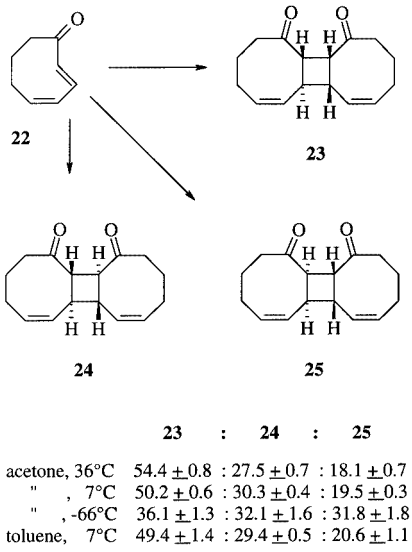

Scheme 10

In the presence of spin = 1/2 agents, **14*a*** and **15*a*** are converted from their singlet states into their triplet states, which, after crossing analogous barriers, also form the final dimers. Structures **14*a*** and **15*a*** can be trapped by nitroxyls and dioxygen to form adducts. A small proportion of the final dimers **11**−**13**, however, is formed without inhibition by nitroxyls and dioxygen; this proportion cannot therefore be formed via **14*a*** and **15*a***. Concerted formation of **12** + **13** is ruled out by orbital symmetry. Hence, this "untrappable" proportion of the dimers must be formed by combination of two molecules of **9** to form the *gauche* 1,4-diradicals **14*g*** and **15*g*** directly. Among these directly formed *gauche* 1,4-diradicals, **15*g*12** (the conformer of **15** that ring-closes to form **12**) is formed in the smallest amount while the other two are formed in roughly equal quantities; the reason for this is that the two radical p-orbitals point towards each other, and thus produce adverse orbital symmetry effects, more strongly in **15*g*12** than they do in the other two *gauche* 1,4-diradicals **14*g*** and **15*g*13** (Scheme 4). The Arrhenius energy of activation for the formation of the "untrappable" share of **13**, and thus for the direct formation of **15*g*13** from **9**, is higher by 2.75 ± 0.44 kcal·mol^{-1} than that for the formation of the "trappable" bulk of **11**, and thus for the formation of **14*a*** from **9** (Figures 2 and 3), and higher by 2.57 ± 0.42 kcal·mol^{-1} than that for the formation of "trappable" **12** + **13**, and thus for the formation of **15*a*** from **9** (Figures 3 and 6).

The Thermal [2+2] Cyclodimerisation of (2*E*,4*Z*)-2,4-Cyclooctadienone (22)

Lange and Neidert reported the isolation of two [2+2] cyclodimers formed thermally from **22** [prepared in situ by UV irradiation of its (*Z*,*Z*) isomer] and established structures **23** and **24** for the major and minor dimer, respectively (Scheme 10). Either dimer was epimerised by strong base to **25**.[69] We studied this dimerisation by carrying out the UV irradiation of the (*Z*,*Z*) isomer in NMR tubes and determining the dimer ratios quantitatively by ^{1}H NMR analysis immediately after each irradiation. We found **25** to be a third dimer formed directly from **22**, and not by epimerisation, in relative amounts as shown in Scheme 10. The ratios given in Scheme 10 were independent of reaction time and of degree of conversion. The dimer distribution obtained from **22** thus turned out to be entirely analogous to that obtained from **9**. Obviously, **22** dimerises via bis(allylic) 1,4-diradicals analogous to **14** and **15**.[34,35] The thermal [2+2] cyclodimerisation of (*E*)-2-cyclooctenone,[70] by contrast, affords an entirely different dimer distribution equally encompassing head-to-head and head-to-tail dimers.[71]

Elucidation of Molecular Structures − Synthetic Aspects

All new compounds afforded the expected analytic, IR, UV, and ^{1}H and ^{13}C NMR spectroscopic data. Molecular masses were determined by CID mass spectrometry, with NH_3 as the reactant gas.

Independent syntheses of **11** and **16** were carried out as outlined in Scheme 11. The molecular structure of diketone

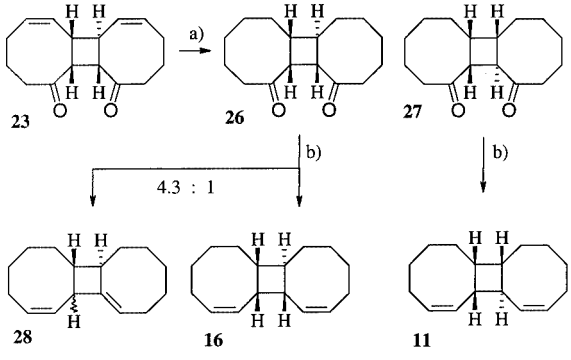

Scheme 11

23 is firmly established.[69] Diketone **27** was obtained by thermal dimerisation of *trans*-cycloct-2-en-1-one;[70,71] its molecular structure has been established by X-ray crystallography.[72]

The molecular structures of the nitroxyl 2:2 adducts (Scheme 5) have been established by four lines of evidence:

i. The molecular structures of adducts **19a/21a** and **20a*u*20a** have been established by X-ray crystallography (Figures 7 and 8, respectively).

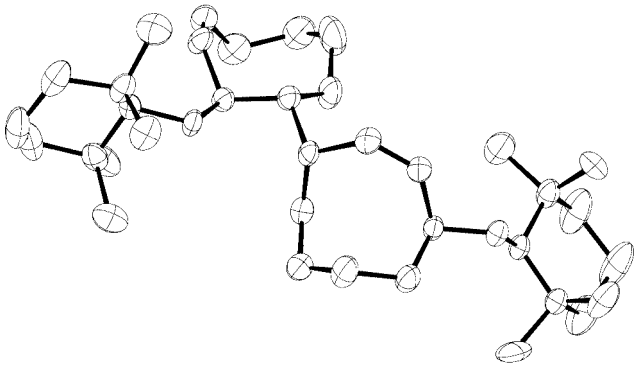

Figure 7. Molecular structure of **19a/21a**; anisotropic displacement parameters are shown at 30% probability level, hydrogen atoms have been omitted for clarity

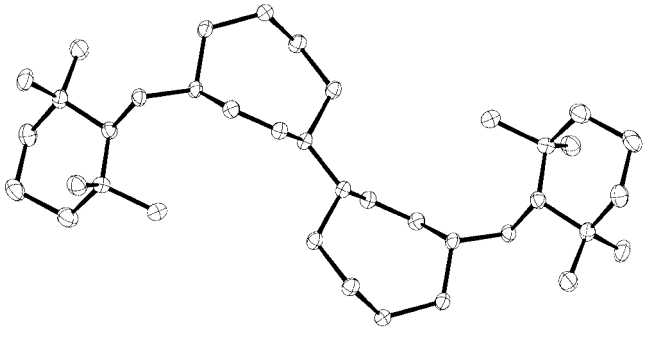

Figure 8. Molecular structure of **20a*u*20a**; anisotropic displacement parameters are shown at 50% probability level, hydrogen atoms have been omitted for clarity

ii. On heating to 110 °C, the adducts isomerise by C−O cleavage to generate a nitroxyl/allyl radical pair followed by recombination.[73] Table 8 summarises such thermolysis experiments. Under forcing thermolysis, all *u* adducts ultimately form mixtures consisting predominantly of **20a*u*20a** or **20b*u*20b**, respectively, and all *l* adducts ultimately form mixtures consisting predominantly of **20a/20a** or **20b/20b**, respectively. This, in combination with the two X-ray-derived structures, allows the assignment of any one 2:2 adduct to *u* or *l*.

iii. Adducts were subjected to the two-step degradation procedure outlined in Scheme 12. This procedure afforded three kinds of information: a) assignment of adducts to *u* or *l*, alternative to thermolysis, b) correlation of **a** adducts with their **b** analogues, and c) proof that the adducts contained C−O bonds throughout and no amine *N*-oxide moieties.[73]

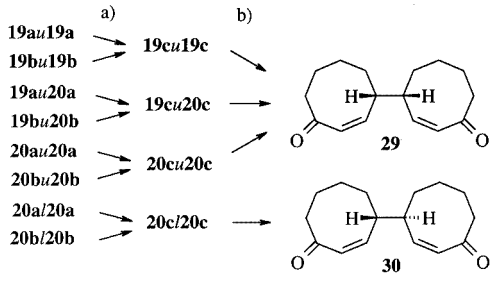

a) Zn powder, glacial acetic acid, 35°C
b) Pyridinium dichromate, dichloromethane

Scheme 12

iv. Table 9 summarises selected ^{1}H NMR spectroscopic data for the nitroxyl adducts, obtained at 270 MHz with the aid of spin decoupling. These data are sufficiently characteristic for the moieties **19**, **20** and **21** to allow the identification of these moieties in the individual adducts. ^{1}H NMR resonances not contained in Table 9 occur at the expected positions.

The principal product formed on dimerisation of **9** in the presence of high concentrations of **18** was **19a*u*19a**. On the other hand, after prolonged heating of the crude reaction product, **20a*u*20a** became its principal constituent. Both **19a*u*19a** and **20a*u*20a** could be isolated by crystallisation from the respective crude reaction products. Since they

Table 8. Thermal isomerisation of 2:2 adducts of **18** at 110 ± 5°C in the presence of 10 % added **18**

Starting adduct	Reaction time/h	% in product mixture (excluding **18**)				
		19a*u*21a	**19a*u*19a**	**19a*u*20a**	**20a*u*20a**	X[a]
19a*u*19a	5	2	24	35	29	10
19a*u*20a	8			30	60	10
19a*u*21a	8			25	40	35
		19a/21a	**19a/19a**	**19a/20a**	**20a/20a**	X[a]
19a/19a	8		10	20	55	15
19a/21a	5	6	27	39	21	7
19a/21a	8		5	15	75	5
21a/21a	8		17	17	50	16

[a] Unidentified products.

Table 9. ^{1}H NMR data ($CDCl_3$) for positions 1−4 of underscored rings of 2:2 adducts of **17** and **18** (position 1 = junction between the two cyclooctene rings)

Position	1	2	3	4	1,2	1,3	2,3	2,4	3,4	4,5	4,5
Adduct		δ/ppm					*J*/Hz (absolute values, ± 0.5)				
19a*u***19a**	2.30	5.43	5.51	4.78	4.8	0.5	12.5	0.5	6.0	5.5	9.5
19a/19a	2.26	5.36	5.48	4.85	4.5	1.0	12.0	0	6.0	6.0	9.5
19a*u***20a**	2.53	5.25	5.63	4.50	7.8	0.5	12.0	0	7.0	2.0	8.0
19a/20a	2.35	5.39	5.60	4.75	6.0	1.5	12.5	1.0	6.5	5.0	10.0
19a*u***21a**	2.90	5.72	5.45	4.99	4.4	2.0	13.0	1.5	6.5	6.0	10.0
19a/21a	2.85	5.31	5.45	4.99	4.0	2.0	13.0	1.0	6.5	6.0	10.0
19aOTEMP	4.65	5.63	5.63	4.65	6.8	1.0	12.2	1.0	6.8	4.8	9.2
19b*u***19b**	2.31	5.38	5.55	4.76	5.0	0.5	12.5	0.5	6.5	5.0	10.0
19b/19b	2.32	5.37	5.58	4.85	4.5	1.0	12.5	1.0	6.0	5.5	10.0
19b*u***20b**	2.51	5.27	5.70	4.52	7.7	1.0	12.0	0.5	6.7	3.7	9.1
19b*u***21b**	−	5.71	5.53	5.04	3.5		12.5	1.0	6.0		
19b/21b	2.89	5.29	5.48	5.03	4.0	2.0	12.5	1.5	6.5	8.0	11.0
20a*u***19a**	2.14	5.26	5.54	4.51	9.0	0	11.0	1.5	8.0	4.5	12.0
20a/19a	2.22	5.41	5.53	4.52	9.0	0	11.0	0	7.5	5.0	12.0
20a*u***20a**	2.08	5.15	5.56	4.49	8.4	0	11.0	1.2	7.8	4.8	10.8
20a/20a	2.19	5.28	5.56	4.49	8.5	0	11.0	1.5	7.8	4.5	11.0
20aOTEMP	4.44	5.54	5.54	4.44	8.0	1.5	11.3	1.5	8.0	5.0	10.8
20b*u***19b**	2.18	5.26	5.66	4.58	9.2	0	11.0	1.5	8.0	4.2	11.4
20b*u***20b**	2.11	5.16	5.68	4.56	8.0	0	11.0	1.0	8.0	4.0	11.0
20b/20b	2.22	5.28	5.68	4.57	8.5	0	11.0	1.0	8.0	4.5	11.0
21a*u***19a**	1.50	4.75	5.96	5.53	10.2	0	7.8	1.2	11.0	Σ =	17.0
21a/19a	1.80	4.68	6.00	5.57	10.0	0	8.0	1.0	11.0	Σ =	17.0
21a/21a	2.32	4.67	6.03	5.45	10.0	0	7.5	1.5	11.0	7.0	9.5
21aOTEMP	4.14	4.84	5.89	5.74	8.5	0	8.5	0	11.0	8.0	8.0
21b*u***19b**	−	4.73	6.17	5.53	10.0	0	9.0		11.5		
21b/19b	−	4.62	6.14	5.47	10.0	0	7.5	1.5	11.5		

could readily be reduced to the respective diols (Scheme 12), the dimerisation of **9** in the presence of **18** (or, alternatively, **17**) offers an efficient route, optionally to diol **19c***u***19c** or to diol **20c***u***20c**, from the commercially available (*Z*,*Z*)-cycloocta-1,3-diene.

Conclusion

The thermal [2+2] cyclodimerisation of (*E*,*Z*)-cycloocta-1,3-diene (**9**) to give the cyclobutanes **11**, **12**, and **13** occurs in two strictly separated steps. In the first step, the first new C−C bond between the two monomer molecules is formed to furnish the singlet *anti* 1,4-diradicals **14*a*** and **15*a***, which are stable species with lifetimes of about 0.5 μs. In the second step, the second new C−C bond is formed after an *anti*-to-*gauche* conformational change of the diradicals. Diradicals **14*a*** and **15*a*** can be chemically trapped by adduct formation with added nitroxyls and with atmospheric dioxygen. Moreover, they are converted into their triplet spin states by added spin = 1/2 species. The two *anti*-to-*gauche* rotational barriers (giving rise to **12** and to **13**, respectively) for **15** have quite different relative heights in the singlet and in the triplet spin states. The kinetics and energetics of the involved reaction steps have been determined (Scheme 9); they are quite different from those of the butadiene parent system and its dimers.

Besides this main path, there is a side path for [2+2] cyclodimerisation of **9** that does not involve **14*a*** and **15*a*** but produces the singlet *gauche* 1,4-diradicals directly from 2 × **9**. These singlet *gauche* diradicals are not trapped by nitroxyl or by dioxygen. The directly formed singlet *gauche* diradical produced in the smallest amount is the one affording **12**, **15*g*12**, which of all the *gauche* diradicals is the one with its two p-orbitals pointing towards each other the most pronouncedly, thus creating adverse Woodward−Hoffmann effects. The energy of activation for direct formation of **15*g*13** from **9** is higher than those for formation of **14*a*** and of **15*a*** from **9** by 2.75 ± 0.44 and 2.57 ± 0.42 kcal·mol^{-1}, respectively.

Experimental Section

General Methods: Melting points: Kofler hot stage, values uncorrected. IR and UV spectra: Perkin−Elmer instruments. ^{1}H and ^{13}C NMR spectra: Bruker WH 270 and AM 400 instruments. Elemental analyses: H. Kolbe, Postfach 100408, 45404 Mülheim a. d. Ruhr, Germany. Preparative liquid chromatography: ambient pressure: silica gel 60 Merck, 0.04−0.063 mm, *n*-pentane + few % ether as the eluent; medium pressure: silica gel HF 10−40 μ Merck, *n*-pentane, peristaltic pump. Preparative GLC: 400 × 2^2 cm^3 20% OV-17 on Chromosorb P, 60−80 mesh, 210 °C, 0.18 mL dimer mixture per cycle. Di-*tert*-butylaminooxyl (**17**)[76] and *N*,*N*′-diisopropylbenzene-1,4-diamine[77] were prepared according to the literature. Compound **17** was purified by distillation through a Vigreux column at 15 mbar. All other reagents were of the highest purity available from Merck, Fluka, and Aldrich and were used as received. Solvents: Merck, analytical grade.

Reagents and Solvents

(*E,Z*)-Cycloocta-1,3-diene (9): Prepared by UV irradiation (immersion well Solidex glass irradiation apparatus, Philips HPK 125 medium-pressure mercury lamp, 125 W, $\lambda > 300$ nm) of the commercially available (*Z,Z*) isomer (60 g, 0.55 mol) in the presence of acetophenone (2 g) in *n*-pentane (600 mL) under argon at −5 °C for 20 h[31] and purified according to a published procedure.[74] It was stored as its crystalline silver nitrate complex[74] at −70 °C. Immediately before use, it was liberated from this complex by aqueous sodium cyanide and distilled from a piece of sodium at 35 °C and 15 mbar into a receiver cooled to −70 °C, purity > 99% (GLC).

Bis[2-(2-ethylhexyl)cyclohexane-1,1′-dionato]copper(II) (Cu): A solution of 2-(2-ethylhexanoyl)cyclohexanone[75] (28.5 g, 127 mmol) in ether (120 mL) was shaken vigorously with a solution of copper(II) sulfate pentahydrate (15.9 g, 64 mmol) and sodium acetate (8.7 g, 128 mmol) in water (120 mL) in a separating funnel for 30 min. The ether layer turned dark green. The residue from the dried ether layer was separated by distillation into unchanged dione (20.8 g, bp. 90 °C/0.015 mbar) and crude **Cu**, which remained as the residue. The unchanged dione, dissolved in ether, was again shaken with the aqueous layer, and the entire procedure was repeated several times with occasional addition of more copper sulfate and sodium acetate. The collected crude **Cu** was crystallised from 50 mL of methanol at −70 °C and the solid was collected by inverse filtration and dried at 0.015 mbar. Dark green powder. $C_{28}H_{46}CuO_4$ (510.21): calcd. C 65.92, H 9.09, Cu 12.45; found C 65.73, H 9.02, Cu 12.15.

Preparative-Scale Dimerisation of 9: Identical mixtures of dimers **11**, **12**, and **13** were prepared either by UV irradiation of (*Z,Z*)-cycloocta-1,3-diene as described above, but at 60 °C in *n*-heptane,[33] or by allowing neat **9** to stand at ambient temperature for several days. Preparative GLC separated these mixtures into (consecutively) **12**, **13**, and **11** (purity 94%, 84%, and 96%, respectively). Crystallisation afforded **12**, m.p. 34−36 °C [ref.[33] 34−35 °C; from ether/hexane (1:3) at −70 °C; 99.7% pure], **13**, m.p. 31−36 °C (from ether at −70 °C; 96.7% pure) and **11**, m.p. 6 °C (from hexane at −70 °C; 99% pure).

Preparative-Scale Dimerisation of 9 in the Presence of 2,2,6,6-Tetramethylpiperidin-1-oxyl (18). (1*S,1′*R**,4*S**,4′*R**)-, (1*S**,1′*S**,4*S**,4′*S**)-, (1*S**,1′*S**,4*S**,4′*R**)-, (1*S**,1′*R**,4*S**,4′*S**)-(*Z,Z*)-4,4′-Bis(2,2,6,6-tetramethylpiperidin-1-yloxy)bicyclooctyl-2,2′-diene (19a*u*19a, 19a/19a, 19a/20a, 19a*u*20a), (1*S**,1′*R**,2′*S**,4*S**)-, (1*S**,1′*S**,2′*R**,4*S**)-(*Z,Z*)-4,2′-Bis(2,2,6,6-tetramethylpiperidin-1-yloxy)bicyclooctyl-2,3′-diene (19a/21a, 19a*u*21a), (1*R**,1′*R**,2*S**,2′*S**)-(*Z,Z*)-2,2′-Bis(2,2,6,6-tetramethylpiperidin-1-yloxy)-bicyclooctyl3,3′-diene (21a/21a), *seqtrans*-, *seqcis*-(*Z*)-3,8-Bis-(2,2,6,6-tetramethylpiperidin-1-yloxy)cyclooctene (19aOR, 20aOR), *seqtrans*-(*Z*)-3,4-Bis(2,2,6,6-tetramethylpiperidin-1-yloxy)cyclooctene (21aOR), (*Z,Z*)-5-(2,2,6,6-Tetramethylpiperidin-1-yloxy)cycloocta-1,3-diene:** A liquid mixture of **9** (13.00 g, 120 mmol) and **18** (20.00 g, 128 mmol) was left standing at room temperature (ca. 22 °C) under argon for 13 d. The mixture became crystalline. Dissolution in *n*-hexane (160 mL) at 40 °C, addition of ethanol (50 mL) and crystallisation at −23 °C furnished **19a*u*19a** (16.00 g, 50%), m.p. 119−125 °C, colourless, pure according to ^{1}H NMR; after several recrystallisations, m.p. 122−126 °C. $C_{34}H_{60}N_2O_2$ (528.86): calcd. C 77.22, H 11.43, N 5.30; found C 77.17, H 11.19, N 5.48. Partial evaporation of the mother liquor to 150 mL and crystallisation at −23 °C afforded a colourless 2:1 (mol/mol) mixture (4.8 g) of **19a**OR (OR = **18**) and **19a*u*19a**, which was separated into the pure components by ambient pressure liquid chromatography, with **19a**OR (m.p. 108−109 °C; $C_{26}H_{48}N_2O_2$ (420.68): calcd. C 74.23, H 11.50, N 6.66; found C 74.19, H 11.60, N 6.75) eluting earlier. Complete removal of all solvent from the mother liquor, addition of ether (15 mL) and crystallisation at room temperature furnished **19a/21a** (950 mg, 93% pure), m.p. 144−154 °C, colourless, after recrystallisation from *n*-pentane at −23 °C, pure **19a/21a** (640 mg), m.p. 153−156 °C. $C_{34}H_{60}N_2O_2$ (528.86): calcd. C 77.22, H 11.43, N 5.30; found C 77.40, H 11.33, N 5.46. The non-crystallising residue (11.2 g) upon fast ambient pressure liquid chromatography (150 g silica gel, pentane + 5% ether) consecutively gave a mixture of dimers **11**, **12**, and **13** (410 mg), overlapping fractions A−C (9.8 g), and **18** (1.0 g). Fraction A (119 mg) on crystallisation from ether at −23 °C furnished pure **21a/21a** (24 mg), m.p. 156−158 °C. $C_{34}H_{60}N_2O_2$ (528.86): calcd. C 77.22, H 11.43, N 5.30; found C 77.23, H 11.36, N 5.26. Fraction B (500 mg) on crystallisation from 15 mL of pentane at −23 °C furnished **19a/21a** (295 mg, 85% pure, vide supra). The mother liquor of fraction B was combined with fraction C and the mixture (9.4 g) was subjected to slow chromatography (300 g silica gel, pentane + 1% ether) to afford consecutively 73 mg unidentified, 8969 mg overlapping fractions D−K (15 mg fraction D, 366 mg fraction E, 3306 mg fraction F, 744 mg fraction G, 1605 mg fraction H, 2741 mg fraction I, 81 mg fraction J, 111 mg fraction K), 178 mg fraction L and 450 mg fraction M. Fraction M consisted mainly of monooxygenated 2:2 adducts according to mass spectrometry. Fraction L was divided into pure **20a**OR (136 mg), m.p. 33−44 °C, colourless [$C_{26}H_{48}N_2O_2$ (420.68): calcd. C 74.23, H 11.50, N 6.66; found C 74.56, H 11.57, N 6.57], followed by 42 mg containing 66% **20a**OR. Fraction E was separated (ether, −23 °C) into 134 mg of crystalline mixture and 232 mg of mother liquor. The latter was combined with fraction D and with the mother liquor of fraction A and on medium pressure chromatography (37 g silica gel) afforded consecutively (*Z,Z*)-5-RO-cycloocta-1,3-diene (5.7 mg), 48 mg of a mixture of (*Z,Z*)-5-RO-cycloocta-1,3-diene and **21a/21a** (vide supra), 40 mg 90% **21a/21a**, 73 mg 70% **19a**OR (vide supra), 74 mg 60% **19a*u*21a**, 20 mg unidentified. The fraction enriched in **19a*u*21a** on crystallisation (pentane, −23 °C) afforded **19a*u*21a**, m.p. 119−128 °C, pure according to ^{1}H NMR. $C_{34}H_{60}N_2O_2$ (528.86): calcd. C 77.22, H 11.43, N 5.30; found C 77.30, H 11.53, N 5.39. Fraction H was separated by crystallisation (ether, −23 °C) into 923 mg of a crystalline mixture of **19a/19a** and **19a*u*19a** (7:3) and 682 mg of mother liquor (fraction N). Several recrystallisations of the crystalline mixture (ether, −23 °C) afforded pure (^{1}H NMR) **19a/19a**, m.p. 121−127 °C, colourless. $C_{34}H_{60}N_2O_2$ (528.86): calcd. C 77.22, H 11.43, N 5.30; found C 77.30, H 11.35, N 5.54. Fraction N on medium pressure chromatography (100 g silica gel) afforded consecutively 227 mg of a mixture of **19a**OR, **19a/21a**, and **19a*u*21a** (vide supra), 13 mg of a mixture of 30 mg 40% **21a**OR, 34 mg 90% **19a/20a** [$C_{34}H_{60}N_2O_2$ (528.86): calcd. C 77.22, H 11.43, N 5.30; found C 77.30, H 11.40, N 5.43], 100 mg of a mixture of **19a/20a** and **19a/19a**, and 273 mg of pure **19a/19a** (vide supra). Fraction J on crystallisation (ether, −23 °C) afforded pure (^{1}H NMR) **19a*u*20a** (21 mg), m.p. 113−119 °C. $C_{34}H_{60}N_2O_2$ (528.86): calcd. C 77.22, H 11.43, N 5.30; found C 77.12, H 11.42, N 5.26. Fraction F, G and I were also separated into fractions and pure adducts by crystallisation. Quantitative 270 MHz ^{1}H NMR analysis of all adduct fractions obtained in this entire experiment, with reference to the ^{1}H NMR spectra of the pure compounds, allowed the establishment of the material balance presented in Table 2. (*Z,Z*)-5-RO-cycloocta-1,3-diene was purified by Kugelrohr distillation (130 °C bath, 0.015 mbar). ^{1}H NMR ($CDCl_3$): δ = 1.10 (s, 12 H), 1.28 (m, 1 H, 6-H), 1.34 (m, 1 H, 7-H), 1.43 (br. s, 6 H), 1.85 (dtdd, *J* = 11, 2 × 10, 4, and 2 Hz, 1 H, 7-H), 2.04 (m, *J* = 16, 6.5, 2, 1.7,

and *x* Hz, 1 H, 8-H), 2.08 (m, 1 H, 6-H), 2.21 (ddddd, J = 16, 10, 5, 2, and 1.7 Hz, 1 H, 8-H), 4.46 (dddd, J = 10.5, 7, 3.5, and 1 Hz, 1 H, 5-H), 5.57 (ddd, J = 11, 6.5, and 5 Hz, 1 H, 1-H), 5.64 (dd, J = 11 and 7 Hz, 1 H, 4-H), 5.74 (ddt, J = 11, 4, and 2 × 1.7 Hz, 1 H, 2-H), 5.82 (ddd, J = 11, 4, and 1 Hz, 1 H, 3-H).

Preparative-Scale Dimerisation of 9 in the Presence of Di-*tert*-butylaminooxyl (17). (1*S,1′*R**,4*S**,4′*R**)-, (1*S**,1′*S**,4*S**,4′*S**)-, (1*S**,1′*R**,4*S**,4′*S**)-(*Z*,*Z*)-4,4′-Bis(di-*tert*-butylaminyloxy)bicyclooctyl-2,2′-diene (19b*u*19b, 19b/19b, 19b*u*20b), (1*S**,1′*R**,2′*S**,4*S**)-4,2′-(*Z*,*Z*)-Bis(di-*tert*-butylaminyloxy)bicyclooctyl-2,3′-diene (19b/21b):** A liquid mixture of **9** (4.00 g, 37 mmol) and di-*tert*-butylaminoooxyl (**17**, 7.80 g, 54 mmol) was left standing at ambient temperature for 12 d. All material volatile below 40 °C at 0.015 mbar was removed by distillation at 40 °C (bath temperature). Crystallisation (pentane/ethanol, −23 °C) afforded **19b*u*19b** (3.76 g, 40%), m.p. 81−84 °C. $C_{32}H_{60}N_2O_2$ (504.84): calcd. C 76.13, H 11.98, N 5.55; found C 76.09, H 11.99, N 5.60. The mother liquor was separated analogously to the procedure above to afford **19b/19b**, m.p. 103−122 °C (purity 90%; $C_{32}H_{60}N_2O_2$ (504.84): calcd. C 76.13, H 11.98, N 5.55; found C 76.29, H 11.86, N 5.70), **19b/21b**, m.p. 120−124 °C [$C_{32}H_{60}N_2O_2$ (504.84): calcd. C 76.13, H 11.98, N 5.55; found C 76.26, H 11.86, N 5.80], and **19b*u*20b**, m.p. 98−100 °C [$C_{32}H_{60}N_2O_2$ (504.84): calcd. C 76.13, H 11.98, N 5.55; found C 76.16, H 12.13, N 5.61]. In addition, one fraction contained 40% **19b*u*21b**.

Preparative-Scale Dimerisation of 9 in the Presence of Di-*tert*-butylaminoooxyl (17) with Workup at 140 °C. (1*S,1′*R**,4*R**,4′*S**)-, (1*S**,1′*S**,4*R**,4′*R**)-Bis(di-*tert*-butylaminyloxy)bicyclooctyl-2,2′-diene (20b*u*20b, 20b/20b):** A liquid mixture of **9** (2.00 g, 18.5 mmol) and **17** (3.90 g, 27 mmol) was left standing at ambient temperature for 12 d. All material volatile at 140 °C and 0.015 mbar was distilled off. Crystallisation of the pale viscous residue from hexane (30 mL) plus ethanol (10 mL) at −23 °C furnished **20b*u*20b** (2.03 g, 43%), m.p. 159−161 °C. $C_{32}H_{60}N_2O_2$ (504.84): calcd. C 76.13, H 11.98, N 5.55; found C 76.23, H 11.87, N 5.60. The residue (1.75 g) on ambient pressure chromatography (400 g silica gel, pentane + 2% ether) afforded consecutively 490 mg containing 25% **20b*u*20b** (rest unknown), 67 mg containing 50% **20b*u*20b** (rest unknown), 138 mg containing 35% **20b*u*20b**, 35% **19b*u*20b**, 15% **19b*u*19b**, and 15% unknown, and pure **20b/20b** (574 mg), after crystallisation (pentane, ethanol, −23 °C) 420 mg, m.p. 98−102 °C [$C_{32}H_{60}N_2O_2$ (504.84): calcd. C 76.13, H 11.98, N 5.55; found C 76.26, H 11.95, N 5.63], and 204 mg unknown.

Preparative Thermal Rearrangements of Adducts: A 10:1 (w/w) mixture of adduct and the corresponding nitroxyl was heated at 110 °C for 5−16 h in a closed vessel.

(1*S,1′*R**,4*R**,4′*S**)-(*Z*,*Z*)-4,4′-Bis(2,2,6,6-tetramethylpiperidin-1-yloxy)bicyclooctyl-2,2′-diene (20a*u*20a):** From either **19a*u*19a**, **19a*u*20a**, or **19a*u*21a**, by crystallisation of the crude reaction mixture (pentane/ether, −23 °C), m.p. 188−189 °C. $C_{34}H_{60}N_2O_2$ (528.86): calcd. C 77.22, H 11.43, N 5.30; found C 77.30, H 11.38, N 5.28.

(1*S,1′*S**,4*R**,4′*R**)-(*Z*,*Z*)-4,4′-Bis(2,2,6,6-tetramethylpiperidin-1-yloxy)bicyclooctyl-2,2′-diene (20a/20a):** From either **19a/19a**, **19a/21a**, or **21a/21a**, by crystallisation of the crude reaction mixture (pentane/ether, −23 °C), m.p. 112−116 °C. $C_{34}H_{60}N_2O_2$ (528.86): calcd. C 77.22, H 11.43, N 5.30; found C 77.24, H 11.23, N 5.43.

***seqcis*-(*Z*)-3,8-Bis(2,2,6,6-tetramethylpiperidin-1-yloxy)cyclooctene (20aOR):** From **19a**OR (494 mg). Ambient pressure chromatography (100 g silica gel, pentane + 0.5% ether) afforded consecutively 73.8 mg of mixtures and **20a**OR (400 mg, 81%), m.p. 33−44 °C (vide supra), pure according to ^{1}H NMR.

Degradation of Adducts According to Scheme 11. (1*S,1′*R**,4*S**,4′*R**)-, (1*S**,1′*R**,4*S**,4′*S**)-, (1*S**,1′*R**,4*R**,4′*S**)-, (1*S**,1′*S**,4*S**,4′*S**)-(*Z*,*Z*)-Bicyclooctyl-2,2′-diene-4,4′-diol (19c*u*19c, 19c*u*20c, 20c*u*20c, 19c/19c), *u*-, *l*-(*Z*,*Z*)-Bicyclooctyl-2,2′-diene-4,4′-dione (29, 30):** Zinc powder (6.00 g, 91 mmol) was added to a solution of **19a*u*19a** (2.00 g, 3.78 mmol) in glacial acetic acid (40 mL) and the slurry was stirred for 6 h at 35 °C[78] in a vessel that allowed the escape of gas. Water (300 mL) was added at room temperature, and the mixture was extracted several times with ether. The combined ether phases were washed successively with water and aqueous sodium bicarbonate solution until they were free of acid. Drying with sodium sulfate and concentration left 917 mg of a crystalline residue, which was dissolved in 220 mL of ether with warming. After concentration to 70 mL, the solution at −23 °C deposited **19c*u*19c** (750.8 mg, 79%), m.p. 143−148 °C, colourless, 95% pure. ^{1}H NMR ($CDCl_3$): δ = 1.3−1.7 (m, 14 H), 1.74 (m, 4 H), 2.57 (m, 2 H), 4.72 (q, J = 3 × 6.0 Hz, 2 H), 5.40 (dd, J = 12.3, 6.0 Hz, 2 H), 5.55 (dd, J = 12.3, 6.0 Hz, 2 H). The same compound, m.p. 144−148 °C, was analogously obtained from **19b*u*19b** (77% yield). Analogously, both **19a*u*20a** and **19b*u*20b** afforded **19c*u*20c**, m.p. 166−175 °C (50% yield) and m.p. 163−177 °C (66% yield), respectively. ^{1}H NMR ($CDCl_3$): δ = 1.1−1.3 (m, 2 H), 1.3−1.78 (m, 14 H), 1.87 (m, 1 H), 1.91 (m, 1 H), 2.19 (dtd; J = 13, 9, 9, 4.5 Hz, 1 H), 2.77 (dtdd, J = 11, 7.5, 7.5, 4.5, 1.5 Hz, 1 H), 4.53 (m, 2 H), 5.26 (ddd, J = 11.5, 10, 2 Hz, 1 H), 5.41 (dd, J = 10.5, 7.5 Hz, 1 H), 5.54 (ddd, J = 10.5, 6.5, 1 Hz, 1 H), 5.68 (ddd, J = 11.5, 6, 1 Hz, 1 H). Analogously, both **20a*u*20a** and **20b*u*20b** afforded **20c*u*20c**, m.p. 230−231 °C, 51% and 33% yield, respectively. ^{1}H NMR ($CDCl_3$): δ = 1.0−1.15 (m, 2 H), 1.3−1.75 (m, 14 H), 1.88 (m, 2 H), 2.19 (dddd, J = 8.5, 7.5, 4, 1 Hz, 2 H), 4.54 (m, 2 H), 5.22 (ddd, J = 11, 9, 2 Hz, 2 H), 5.54 (dd, J = 11, 6.5 Hz, 2 H). Analogously, both **20a/20a** and **20b/20b** afforded **20c/20c**, m.p. 192−199 °C, 23% and 70% yield, respectively. ^{1}H NMR ($CDCl_3$): δ = 1.1−1.25 (m, 2 H), 1.3−1.75 (m, 14 H), 1.87 (m, 2 H), 2.38 (m, 2 H), 4.54 (dddd, J = 11.5, 6.5, 4, 2 Hz, 2 H), 5.27 (ddd, J = 11, 9, 2 Hz, 2 H), 5.55 (dd, J = 11, 7 Hz, 2 H).

Pyridinium dichromate (2.00 g, 5.31 mmol) was added to a solution of **19c*u*19c** (300 mg, 1.2 mmol) in dichloromethane (50 mL) and the mixture was stirred under reflux for 105 min. The reaction mixture was shaken with aqueous sodium hydroxide (10%, 50 mL). The dichloromethane phase was freed of pyridine by washing with aqueous sulfuric acid followed by water. After drying with magnesium sulfate and concentration, 279 mg of a brown solid was left. The solid was treated with ether and the resulting ethereal solution was filtered and concentrated to 40 mL. At −23 °C it deposited **29** (206.2 mg, 70%), off-white, m.p. 131−133 °C. ^{1}H NMR ($CDCl_3$): δ = 1.25−1.4 (m, 2 H), 1.45−1.9 (m, 10 H), 2.51 (dt, J = 14.5, 5.5, 5.5 Hz, 2 H), 2.82 (m, 4 H), 6.09 (quasi-s, 4 H). ^{13}C NMR ([D$_6$]acetone): δ = 23.5 (CH_2), 24.9 (CH_2), 29.5 (CH_2), 43.1 (CH_2), 45.4 (CH), 134.4 (CH), 145.3 (CH), 203.3 (C=O). The same compound was analogously obtained from **19c*u*20c** (mp. 124−135 °C, 50%) and from **20c*u*20c** (m.p. 123−134 °C, 22%). Analogously, **20c/20c** was converted into **30**, m.p. 111 °C, 91% yield. ^{1}H NMR ($CDCl_3$): δ = 1.3−1.45 (m, 2 H), 1.45−1.9 (m, 10 H), 2.50 (dt, J = 14, 5.5, 5.5 Hz, 2 H), 2.82 (ddd, J = 14.5, 10.5, 7 Hz, 2 H), 2.92 (m, 2 H), 6.06 (dd, J = 12.5, 5 Hz, 2 H), 6.13 (bd, J = 12.5 Hz, 2 H). ^{13}C NMR ([D$_6$]acetone): δ = 23.6 (CH_2), 24.8 (CH_2), 29.0 (CH_2), 43.0 (CH_2), 45.3 (CH), 134.0 (CH), 144.8 (CH), 203.5 (C=O).

6a*r*,6b*c*,12a*t*,12b*c*-1,2,3,4,6a,6b,9,10,11,12,12a,12b-Dodecahydrocycloocta[3,4]cyclobuta[1,2][8]annulene (16)

(A) By Thermolysis of 12: Pyrex vessels consisting of a 2-l bulb connected to a closed tube of 5 cm length on one side and an open tube on the opposite side were used. The vessel was charged with pure **12** (100 mg), the closed tube holding **12** was cooled to −70 °C, the vessel was evacuated to 0.015 mbar through the open tube, and the open tube was sealed by a flame. The vessel was placed in an air thermostat heated to 290 °C for 130 min. After cooling to room temperature, the closed tube was immersed into liquid N_2 for several minutes and the vessel was opened at the opposite tube where it had been sealed. The material that had condensed in the closed tube was recovered by dissolution in ether. A total of 85 such runs were carried out. From the combined and concentrated ether solutions, 62% of **12** was recovered by crystallisation at −70 °C. The residue of the mother liquor (2.74 g) consisted of 45% **12**, 10% **13**, 37% **16** and 7.7% of various unidentified GLC peaks. In the gas chromatograms, **16** appeared between **13** and **11**, immediately following **13**. Preparative GLC afforded **16** (647 mg), m.p. 8−10 °C, 95% pure, containing 3.4% **13**. Crystallisation (ether/hexane, −70 °C) furnished 449 mg, m.p. 9−11 °C, 98% pure. $C_{16}H_{24}$ (216.37): calcd. C 88.82, H 11.18; found C 88.26, H 11.80. ^{1}H NMR ($CDCl_3$): δ = 1.16−1.36 (5 H), 1.50 (2 H), 1.64 (1 H), 1.68 (1 H, 12a-H), 1.7−1.8 (4 H), 1.82 (1 H, 12b-H), 1.98−2.10 (2 H, 2 4-H), 2.13 (1 H, 9-H), 2.23 (1 H, 9-H), 2.75 (1 H, 6b-H), 3.24 (1 H, 6a-H), 5.57 (1 H, 8-H), 5.67 (1 H, 6-H), 5.72 (1 H, 7-H), 5.81 (1 H, 5-H); selected *J* values (Hz): 8 (6a-H, 6b-H), 8 (6a-H, 12b-H), 5.4 (6a-H, 6-H), 2.6 (6a-H, 5-H), 11 (6-H, 5-H), 1.8 (6-H, 4-H), 6.6 (5-H, 4-H), 7.1 (5-H, 4-H), 10.3 (6b-H, 12a-H), 4.6 (6b-H, 7-H), 2.3 (6b-H, 8-H), 11.3 (7-H, 8-H), 1.5 (7-H, 9-H), 6 (8-H, 9-H), 9 (8-H, 9-H). ^{13}C NMR ($CDCl_3$): δ = 26.1, 26.6, 27.3, 27.9, 28.2, 29.5, 30.5, 32.5 (8 CH_2), 37.6, 42.3, 48.5, 48.6, 127.1, 128.7, 131.3, 133.5 (8 CH).

Catalytic hydrogenation (Pd/C, ethanol, ambient conditions, uptake 2 mol H_2 per mol **16**) furnished a hydrocarbon identical to that obtained by analogous hydrogenation of **11**.

(B) By Shapiro Reaction[79] from 26. 6a*r*,6b*t*,12a*c*,12b*c*-Tetradecahydrocycloocta[3,4]cyclobuta[1,2][8]annulene-1,12-dione (26): This compound was prepared by catalytic hydrogenation (Pd/C, ethanol, ambient conditions, uptake 2 mol H_2) of **23**.[69] Liquid. ^{1}H NMR ([D_6]acetone): δ = 1.0−1.5 (m, 6 H), 1.5−2.0 (m, 10 H), 2.0−2.22 (m, 2 H), 2.10 (tdd, *J* = 9, 9, 8.5, 3 Hz, 1 H, 6a-H), 2.38 (dtd, *J* = 10.5, 9, 9, 2 Hz, 1 H, 6b-H), 2.40 (m, 1 H), 2.45 (dd, 10.5, 7 Hz, 1 H, 12a-H), 3.26 (td, *J* = 12, 12, 6 Hz, 1 H), 4.02 (dd, *J* = 8.5, 7 Hz, 1 H, 12b-H). **Bis(*p*-toluenesulfonyl) Hydrazone:** Concd. aqueous HCl (0.1 mL) was added at room temperature whilst stirring to a solution of **26** (1.50 g, 6 mmol) and *p*-toluenesulfonyl hydrazide (2.50 g, 13.4 mmol) in methanol (14 mL). The mixture became slightly warm. After 1 h, the mixture was cooled to 0 °C and 3.5 g of a colourless precipitate was collected, to afford after recrystallisation (200 mL of methanol, cautious warming, concentration of the solution in vacuo to 70 mL, −23 °C) 2.35 g (66%), m.p. 129−131 °C. $C_{30}H_{40}N_4O_4S_2$ (584.79): calcd. C 61.61, H 6.89, N 9.58, O 10.94, S 10.97; found C 61.35, H 7.15, N 9.43, O 11.09, S 10.84. *Caveat:* Prolonged reaction time or too strong heating during recrystallisation caused epimerisation to the bis(*p*-toluenesulfonyl hydrazone) of the hydrogenation product of **25**, m.p. 182−186 °C. **Mixture of 28 and 16:** The bis(hydrazone) (6.30 g, 10.8 mmol) was suspended under argon in anhydrous ether (95 mL). Methyllithium in ether (1.6 N, 35 mL, 56 mmol) was added dropwise with stirring below 25 °C. Stirring under argon at room temperature was continued for 15 h to give an orange solution. After aqueous workup under argon, the ether solution left 3.2 g oily yellow residue. This, on Kugelrohr distillation (150 °C bath, 0.015 mbar), furnished 0.76 g of a distillate. Ambient pressure chromatography (80 g of silica gel; pentane) of the distillate gave 0.56 g of a first fraction, which was distilled (100 °C bath, 0.015 mbar) to afford 0.33 g (14%) of a 4.3:1 mixture of **28** and **16** (GLC, MS). The structure **28** for the major component follows from its ^{1}H NMR spectrum in the mixture. Compound **16** was identified by GLC and by its highly characteristic ^{1}H NMR signature (vide supra) which was only partially obscured by that of **28**.

6a*r*,6b*t*,12a*c*,12b*c*-1,2,3,4,6a,6b,9,10,11,12,12a,12b-Dodecahydrocycloocta[3,4]cyclobuta[1,2][8]annulene (11)

By Shapiro Reaction[79] from 27. 6a*r*,6b*c*,12a*t*,12b*c*-Tetradecahydrocycloocta[3,4]cyclobuta[1,2][8]annulene-1,12-dione (27): This compound was formed (10%) together with regio- and stereoisomers in the course of the thermal dimerisation of (*E*)-cyclooct-2-en-1-one[70,71] in heptane at 25 °C and was isolated by preparative HPLC, m.p. 91−93 °C. ^{1}H NMR ([D_6]acetone): δ = 1.1 (m, 1 H), 1.18−1.40 (m, 3 H), 1.4−2.0 (m, 12 H), 2.10 (m, 1 H), 2.31 (dddd, *J* = 11.3, 10.3, 8.8, 2.8 Hz, 1 H, 6b-H), 2.33 (m, 2 H), 2.55 (dt, 12, 4, 4 Hz, 1 H), 2.73 (dddd, *J* = 11, 9, 8.8, 1.6 Hz, 1 H, 6a-H), 3.49 (dd, *J* = 10.3, 9.5 Hz, 1 H, 12a-H), 3.58 (dd, *J* = 9.5, 9 Hz, 1 H, 12b-H). **Bis(*p*-toluenesulfonyl) Hydrazone:** This compound was prepared from **27** (1.50 g, 6 mmol) as above for **26**, but no precautions against epimerisation were necessary; 3.14 g (89%), m.p. 207−208 °C. $C_{30}H_{40}N_4O_4S_2$ (584.79): calcd. C 61.61, H 6.89, N 9.58, O 10.94, S 10.97; found C 61.77, H 6.74, N 9.61, O 11.00, S 10.90. **Compound 11:** The bis(hydrazone) (6.3 g, 10.8 mmol) treated as above for **26** yielded 2.85 g of residue of the ether layer, which on ambient pressure chromatography gave 1.62 g of a first fraction, the middle cut of which (1.36 g) afforded **11** (1.26 g) on distillation, bp. 80−82 °C/0.1 mbar, 91% pure (49% yield), identical in all respects with the major dimerisation product of **9**. The contaminants were 13 unidentified minor GLC peaks.

Analytic and Kinetic Experiments

General: Quantitative capillary GLC analyses: Several GLC conditions were used with equal success and differed only little in relative retention times for hydrocarbons. The following were typical. 1) 23 m CW-20M, temperature program 70−250 °C with 4 °C/min, injection port 233 °C, 0.4 atm H_2, 0.1 μL injected. Compounds **12**, **13**, **16**, and **11** appeared 33.9, 35.6, 36.1, and 36.7 min, respectively, after injection. 2) 50 m OV-101, temperature program 70−220 °C with 4 °C/min, injection port 200 °C, 0.8 atm H_2, 0.1 μL injected. Compounds **12**, **13**, **16**, and **11** appeared 25.3, 26.4, 26.6, and 26.9 min, respectively, after injection.

Kinetic Experiments: *n*-Octane was distilled from $LiAlH_4$ into a vessel that allowed degassing by freeze-evacuate-thaw-argon cycles and which also allowed addition and removal of contents by syringe through a rubber septum. The distilled *n*-octane was degassed and then stored under argon in this vessel. Immediately before kinetic runs, ca. 3% (relative to **9**) each of *n*-decane, *n*-tetradecane, and *n*-heptadecane, precisely weighed, were added to freshly prepared **9** (vide supra); ca. 3% *N,N′*-diisopropylbenzene-1,4-diamine was also added as a polymerisation inhibitor except for runs in the presence of nitroxyls or transition metal complexes. Weighed solutions of this mixture in *n*-octane were then immediately prepared by syringe techniques in a vessel similar to the one described above, degassed, and stored under argon on ice (solutions "**9**"). Kinetic runs with these solutions were carried out depending on additives as described below. After the desired reaction time, each analytic sample was quenched by addition of sufficient freshly distilled

cyclopentadiene at ambient temperature, which immediately, selectively, and quantitatively converted unchanged **9** into the two Diels−Alder adducts (1.8:1) of cyclopentadiene to the (*E*) double bond of **9** and left all other constituents untouched. Quantitative analyses were carried out by measuring the GLC signal areas of **10** and of (*Z*,*Z*)-cycloocta-1,3-diene relative to *n*-decane, of the two Diels−Alder adducts relative to *n*-tetradecane, and of dimers relative to *n*-heptadecane, using factors determined on weighed mixtures of pure compounds. For every kinetic run, three "zero" analytic samples, using the same batch of reactant solution but quenched after zero reaction time, were taken and analysed, and used as zero time reference. Rates for formation of 2:2 adducts with **17** and of dioxygen trapping products should equal the rates for disappearance of the sum (in terms of C_8 units) of all other significant constituents derived from **9** [i.e., of **9**, **10**, (*Z*,*Z*)-cycloocta-1,3-diene, **11**, **12**, and **13**]; they were determined on this basis. The selection of concentration ranges and reaction times used in the kinetic analyses was governed by the goal of achieving sufficient precision. In view of the achieved precision of the GLC analyses (mostly ca. 3 relative %) this goal was demanding in many of the trapping experiments. In general, reaction times such as to obtain conversions of **9** ranging from 10−50% were chosen.

Kinetic Runs under Argon in the Absence of Additives: Sample tubes (1 mL) were flushed with a stream of argon and closed with rubber septa while still under a stream of argon. By syringe, each tube was charged with solution "**9**" (0.5 mL) and submerged in a water thermostat kept at the desired temperature. After the desired reaction times, the tubes were removed from the thermostat, opened, quenched, and analysed. For each temperature (5, 15, 35, 45 and 55 °C), eight non-zero-time samples using [**9**] = 0.6 M were produced and analysed. For 25 °C, altogether 57 non-zero-time samples spanning [**9**] = 0.136−1.33 M were produced and analysed.

Kinetic Runs in the Presence of 17: Study of the kinetics of nitroxyl addition to diradicals **14** and **15** was rendered difficult by the influence exerted by trace concentrations of atmospheric oxygen. Nitroxyl **18** has been found[80] to react with alkylperoxyl radicals, resulting in liberation of half of the peroxyl oxygen as dioxygen while **18** is regenerated. Consequently, if the alkylperoxyl radicals are formed by trapping of an alkyl radical with dioxygen, the dioxygen liberated may again trap one molecule of alkyl radical. Thus there is a cooperative effect by dioxygen and nitroxyl in trapping alkyl radicals, and this will particularly appear at low nitroxyl concentration, when even traces of dioxygen can compete with nitroxyl for the radicals. When **9** was allowed to dimerise in the presence of varying concentrations of nitroxyl **17** while dioxygen was not excluded rigorously enough, and the resulting values for k_{11}, k_{12} (Table 1) or k_{dim} (Table 3) were plotted vs. [**17**], the plots exhibited a marked discontinuity in that the smooth curves when extrapolated to [**17**] = 0 crossed the ordinate at values one half to one third of the value for ${}_0k$ that was obtained in the absence of **17**. The procedure reported below eliminated the discontinuity and did lift the curves so as to cross the ordinate at ${}_0k$. There was an additional requirement: the change in [**9**] (i.e., $[\mathbf{9}]_0 - [\mathbf{9}]$) during a kinetic run had to be small as compared to [**17**] (a correspondingly averaged [**17**] had to be used to calculate the rate constants from the analyses); this limited the compatible ranges of [**9**], [**17**] and reaction times. Weighed solutions of **17** in *n*-octane were prepared in a vessel that allowed degassing (vide supra) and also allowed addition and removal of contents by syringe through a rubber septum. They were repeatedly degassed, and charged with argon (solutions "**17**"). The reaction vessels for the kinetic runs were 10-mL glass sample tubes prepared as follows. Each tube was completely filled with oxygen-free (vide supra) *n*-octane and closed with a rubber septum; by means of two syringes the *n*-octane inside the tube was replaced by argon; the two syringes were removed and the tubes were stored in a dessicator under argon until use. For one kinetic run, a measured volume of one solution "**17**" and a measured volume of one freshly prepared solution "**9**" (8 mL together) were placed into one tube by syringes and the weight of each added solution was determined by weighing the tube before and after each addition. After a "zero" sample had been taken by means of one syringe while the second syringe admitted argon into the tube, the syringe holes in the rubber septa were sealed with wax and the tube was submerged in a water thermostat kept at 25 °C; after the desired reaction times, analytic samples were taken in the same manner, quenched and analysed. Altogether, 27 non-zero-time samples for [**17**] ≤ 0.105 M and 99 for higher [**17**] were used for kinetic analysis.

Kinetic Runs in the Presence of Oxygen. Under 1 atm of Pure Oxygen: A flat, round-bottomed 50-mL three-necked flask was connected to a gas burette on one neck and to a "gas mouse" on another neck; the central neck was closed by a rubber septum. (A "gas mouse" is a glass bulb with two opposite exit tubes, both of which can be closed by taps.) One exit tube featured a ground joint fitting on one neck of the flask; the other exit tube allowed connection to a vacuum line. The flask was equipped with a magnetic stirring bar and immersed into a water thermostat bath placed above a magnetic stirrer. The system was evacuated to 0.015 mbar through the gas mouse, both taps of the gas mouse were closed, and the flask was charged with "1 atm" (more precisely, the pressure read from the barometer) of pure oxygen through the gas burette. A freshly prepared solution "**9**" (3 mL) was purged with a stream of oxygen and injected by syringe through the rubber septum into the three-necked flask. It was kept there with vigorous stirring for the desired time while the oxygen pressure was kept constant by use of the gas burette. By syringe, analytic samples were drawn after zero time and after the desired reaction times, quenched and analysed. At the end of the run, a sample of the gas inside the flask was drawn into the evacuated gas mouse and analysed by mass spectrometry; the effective oxygen pressure during the reaction was calculated according to this analysis. A total of 4 equivalent runs at a time could be carried out together. **Under 1 atm of Air:** As above for pure oxygen, with the following differences. In addition to the gas burette containing air, a 4-l round-bottomed flask containing air was used; the air contained in it was slowly pumped (by peristaltic pump) through pure *n*-octane contained in a trap kept at the reaction temperature by a thermostat, and thence into the reaction flask, and thence back into the 4-l flask. The gas burette served to keep the pressure constant. The absence of a significant oxygen depletion effect revealed itself by the independence of the observed k_{11}, k_{12} and k_{13} values of [**9**]; in the case of depletion, these values would have increased with [**9**]. Altogether 16, 12, 41, 14, 17, and 18 non-zero-time samples were drawn at 5, 15, 25, 35, 45, and 55 °C, respectively, and used for kinetic analysis.

Saturation Concentration of Oxygen in *n*-Octane between 5 and 55 °C: A 250-ml magnetically stirred, round-bottomed, three-necked flask was equipped with a stop-cock leading to a vacuum line and to an argon supply on the first neck, with a 50-mL graduated dropping funnel allowing the contents to be purged by a stream of argon on the second neck, and a 100-mL graduated dropping funnel carrying an interior thermometer and surrounded by a jacket through which water from a thermostat was pumped, on the third neck. Solution A: 1 L of aqueous solution containing $MnSO_4 \cdot H_2O$ (33.8 g), $FeSO_4 \cdot 7H_2O$ (55.6 g) and concd. HCl (20 g). Solution B: aqueous NaOH (2.5 N). Solution C: aqueous HCl (6 N). All three

solutions were evacuated in an ultrasound bath at 0 °C and charged three times with 1 atm argon. The entire apparatus was evacuated and charged with 1 atm argon. Solution A (50 mL) was transferred into the 50-mL dropping funnel with a pressure line and admitted into the 250-mL flask by applying weak vacuum. In the same way, solution B (20 mL) was added whilst stirring, causing the formation of a pale grey-green precipitate in the 250-mL flask. *n*-Octane was saturated with air at the desired temperature by placing it in a water thermostat and bubbling air through it; slightly more than 100 mL of it was then quickly transferred by means of a voluminous pipette into the 100-mL dropping funnel which was thermostatted to the desired temperature. Its temperature was read there, and exactly 100 mL of it was admitted to the 250-mL flask by applying weak vacuum (some residual *n*-octane must remain in the dropping funnel). The resulting mixture was stirred for 1 h. Solution C (30 mL) was then added in the same way as for solutions A and B, and the mixture was stirred until all precipitates had dissolved. The apparatus was opened, the aqueous phase was collected quantitatively, and sodium iodide (10 g) was dissolved in it. After 10 min in the dark, the liberated iodine was titrated with sodium thiosulfate (0.1 N, "Titriplex" Merck), requiring about 9−11 mL of it. By exactly the same procedure, a blind was carried out using 100 mL of *n*-octane saturated with argon in place of air, and affording a correction (about 0.1 mL) to the value determined above. For every temperature, 6−17 runs were carried out; observed precision 0.5−4 relative %.

Kinetic Runs in the Presence of Cu: Weighed solutions of **Cu** in *n*-octane were prepared, degassed, and stored under argon (solutions "**Cu**") in analogy to solutions "**17**". Sample tubes (2 mL) filled with argon and closed with rubber septa were prepared as above for kinetic runs without additives. Each tube was charged with measured volumes of solutions "**9**", "**Cu**", and of *n*-octane (altogether 1 mL) by syringe and submerged in a water thermostat kept at 25 °C. After the desired reaction times, analytic samples were taken from the tubes, quenched and analysed. Altogether, 73 non-zero-time samples were drawn and analysed.

Kinetic Runs in the Presence of Cobaltocene: Magnetically stirred glass reaction tubes (5 mL) that could be closed by a rubber septum at the top and that carried a side arm with a tap connected to a vacuum and argon line were used. A total of 18 such tubes were immersed together in a water thermostat kept at 25 °C and placed above 3 magnetic stirrers. The open tubes were flushed with argon. A total of 18 lots of cobaltocene crystals were weighed on folded fresh playing cards and filled into the tubes through the top, after which the tubes were tightly closed by the rubber septa, evacuated and charged with argon. With all taps open and a slow stream of argon passing through the entire system, escaping through the syringe holes, each tube was charged with solution "**9**" (3 mL) by syringe and magnetic stirring was commenced. After zero time and after the desired reaction times, analytic samples were taken from each tube, quenched and analysed. A total of 34 analysed non-zero-time samples with [**Co**] ≥ 0.029 M were used for the kinetic analysis; another 36 with lower [**Co**] were not used.

Thermolyses of 12 and 13. Kinetic Runs: The procedure was as in the preparative thermolysis of **12** to give **16** described above, but with 20-mg samples in 250-mL bulbs and restricting conversions to < 7%. For each reaction temperature, 2 runs were performed for a definite time and 2 more runs for twice that time. At the lowest temperature studied (220 °C), 2 more runs were performed at three times that time.

MM3 Calculations: See refs.[24−26] All structures including transition states were refined by full-matrix optimisation and fully characterised by calculated thermodynamic data and IR frequencies (transition states featuring exactly one imaginary frequency). Transition states were tracked down by using the dihedral angle driver feature between the two pertinent energy minima.

Crystal Structure Determination: The intensity data for the compounds were collected with an Enraf−Nonius CAD-IV diffractometer (**19a/21a**) and a Nonius−Kappa CCD diffractometer (**20a*u*20a**), by using graphite-monochromated Mo-K_α radiation. The structures were solved by direct methods (SHELXS-97[81]) and refined by full-matrix, least-squares techniques against F^2 (SHELXL-97[82]). For **19a/21a** the hydrogen atoms were included at calculated positions with fixed thermal parameters, for **20a*u*20a** the hydrogen atoms were located by difference Fourier synthesis and refined isotropically. All non-hydrogen atoms were refined anisotropically. **Crystal Data Collection for 19a/21a:** $C_{34}H_{60}N_2O_2$, M_r = 528.84 g·mol^{-1}, colourless blocks, size 0.43 × 0.25 × 0.14 mm, orthorhombic, space group *Pbca*, a = 16.537(4) Å, b = 17.571(3) Å, c = 22.840(4) Å, V = 6637(2) Å^3, T = 293 K, Z = 8, $\rho_{calcd.}$ = 1.059 g·cm^{-3}, μ (Mo-K_α) = 0.064 mm^{-1}, F(000) = 2352 e, λ = 0.71069 Å, 4563 reflections in h(0/18), k(0/19), l(0/24), measured in the range 1.78° ≤ Θ ≤ 22.91°, 1774 reflections with $I > 2\sigma(I)$, 343 parameters, R_1 = 0.082, wR_2 = 0.259, GOOF = 0.837, largest difference peak and hole = 0.2/−0.2 e·Å^{-3}. **Crystal Data Collection for 20a*u*20a:** $C_{34}H_{60}N_2O_2$, M_r = 528.84 g·mol^{-1}, colourless blocks, size 0.17 × 0.14 × 0.03 mm^3, monoclinic, space group $P2_1/c$, a = 11.4775(4) Å, b = 13.1321(5) Å, c = 10.8253(3) Å, β = 104.980(2)°, V = 1576.18(9) Å^3, T = 173 K, $\rho_{calcd.}$ = 1.114 g·cm^{-3}, Z = 2, μ (Mo-K_α) = 0.068 mm^{-1}, F(000) = 588 e, λ = 0.71069 Å, 11948 reflections in h(−16/15), k(−16/18), l(−15/13), measured in the range 1.84° ≤ Θ ≤ 30.05°, completeness $\Theta_{max.}$ = 95.7%, 4421 independent reflections, 2444 reflections with $I > 2\sigma(I)$, 292 parameters, R_1 = 0.069, wR_2 = 0.201, GOOF = 1.065, largest difference peak and hole = 0.4/−0.4 e·Å^{-3}. Crystallographic data (excluding structure factors) for **19a/21a** and **20a*u*20a** have been deposited with the Cambridge Crystallographic Data Centre as supplementary publication nos. CCDC-175175 (**19a/21a**) and -175174 (**20a*u*20a**). Copies of the data can be obtained free of charge on application to CCDC, 12 Union Road, Cambridge CB2 1EZ, UK [Fax: (internat.) + 44-1223/336-033; E-mail: deposit@ccdc.cam.ac.uk].

Acknowledgments

The authors wish to thank Mrs. Kerstin Sand and Mr. Jörg Bitter for carrying out the NMR experiments and Mrs. Gabriele Schmitz and Mrs. Ursula Westhoff for countless GLC analyses. J. L. and I. H. wish to express their gratitude to the directors of the Institut für Strahlenchemie, Prof. K. Schaffner and the late Prof. O. E. Polansky, for their continuing support.

[1] J. A. Berson, *Science* **1994**, *266*, 1338−1339.
[2] S. Pedersen, J. L. Herek, A. H. Zewail, *Science* **1994**, *266*, 1359−1364.
[3] S. De Feyter, E. W.-G. Diau, A. A. Scala, A. H. Zewail, *Chem. Phys. Lett.* **1999**, *303*, 249−260.
[4] C. Doubleday, Jr., *J. Am. Chem. Soc.* **1993**, *115*, 11968−11983.
[5] C. Doubleday, Jr., *Chem. Phys. Lett.* **1995**, *233*, 509−513.
[6] C. Doubleday, Jr., *J. Phys. Chem.* **1996**, *100*, 15083−15086.
[7] N. W. Moriarty, R. Lindh, G. Karlström, *Chem. Phys. Lett.* **1998**, *289*, 442−450.
[8] W. v. E. Doering, W. R. Roth, F. Bauer, M. Boenke, R. Breuck-

mann, J. Ruhkamp, O. Wortmann, *Chem. Ber.* **1991**, *124*, 1461−1470.
[9] The latter are based on Arrhenius activation energies rather than on Eyring enthalpies of activation and therefore include a thermal energy of *RT*/2 in their reaction coordinate on top of the barrier.
[10] Scheme 2 assumes the interconversions of **5** with **1**, **2** and **3** to occur only via **4**. This assumption is supported by the reasoning that a ring-closure of the *cc-gauche* diradicals (which could ring-close to **5** whereas the *ct-gauche* and *tt-gauche* diradicals **6** could not) should, for reasons of orbital overlap, ring-close to **4** in strong preference to **5**. (This reasoning is *not* contradicted by the equilibrium between **4** and **5**, in combination with the principle of microscopic reversibility.)
[11] W. v. E. Doering, M. Franck-Neumann, D. Hasselmann, R. L. Kaye, *J. Am. Chem. Soc.* **1972**, *94*, 3833−3844.
[12] W. v. E. Doering, D. M. Brenner, *Tetrahedron Lett.* **1976**, 899−902.
[13] For more C_8H_{12} species see: R. Walsh, H.-D. Martin, M. Kunze, A. Oftring, H.-D. Beckhaus, *J. Chem. Soc., Perkin Trans. 2* **1981**, 1076−1083.
[14] Standard heats of formation: **1** (two molecules of butadiene): 52.66;[15] **2**: 42.4;[16] **5**: 25.27;[16] **8**: 37.8;[16] Arrhenius energies: **2a** → **2b**: 36.9 ± 0.9; **2** → **1**: 39.0 ± 0.9; **2** → **3**: 34.5 ± 0.7; **2** → **5**: 35.0 ± 0.7 (all recalculated from ref.[17]); **1** → **3**: 24.53 ± 0.12; **1** → **5**: 28.44 ± 0.1; **5** → **1**: 56.38 ±0.1; **5** → **3**: 51.78 ± 0.12 (all from ref.[18]); **4** → **5**: 24.0 ± 0.14;[17,19] **4** → **8**: 26.3 ± 0.3;[19] **8** → **4**: 32.5 ± 1.0.[19−21] The value for **4** follows from the values for **8**, **4** → **8**, and **8** → **4**.
[15] S. W. Benson, F. R. Cruickshank, D. M. Golden, G. R. Haugen, H. E. O'Neal, A. S. Rodgers, R. Shaw, R. Walsh, *Chem. Rev.* **1969**, *69*, 279−324.
[16] W. R. Roth, O. Adamczak, R. Breuckmann, H.-W. Lennartz, R. Boese, *Chem. Ber.* **1991**, *124*, 2499−2521.
[17] G. S. Hammond, C. D. DeBoer, *J. Am. Chem. Soc.* **1964**, *86*, 899−902.
[18] G. Huybrechts, L. Luyckx, Th. Vandenboom, B. van Mele, *Int. J. Chem. Kinet.* **1977**, *9*, 283−293.
[19] J. Leitich, *Int. J. Chem. Kinet.* **1979**, *11*, 1249−1261.
[20] H.-D. Martin, M. Kunze, H.-D. Beckhaus, R. Walsh, R. Gleiter, *Tetrahedron Lett.* **1979**, 3069−3072.
[21] I. Rencken, S. W. Orchard, *S.-Afr. Tydskr. Chem.* **1988**, *41*, 22−25.
[22] W. R. Roth, V. Staemmler, M. Neumann, C. Schmuck, *Liebigs Ann.* **1995**, 1061−1118.
[23] S. W. Benson, *Thermochemical Kinetics*, 2nd ed., John Wiley, New York, **1976**.
[24] MM3.95, release 1.2: Tripos, Inc., 1699 South Hanley Road, St. Louis, MO 63144, USA.
[25] N. L. Allinger, Y. H. Yuh, J. H. Lii, *J. Am. Chem. Soc.* **1989**, *111*, 8551−8566.
[26] R. Liu, N. L. Allinger, *J. Comp. Chem.* **1994**, *15*, 283−299.
[27] H.-D. Martin, E. Eisenmann, M. Kunze, V. Bonacic-Koutecky, *Chem. Ber.* **1980**, *113*, 1153−1179.
[28] A barrier of ca. 5 kcal·mol^{-1} was obtained by quantum mechanical calculations: Y. Li, K. N. Houk, *J. Am. Chem. Soc.* **1993**, *115*, 7478−7485.
[29] Note that the reaction **1** → **3** is concerted, which depresses its transition state energy from the ≥81.5 kcal·mol^{-1} for **1** → **6** down to the observed 77.2 kcal·mol^{-1}: F.-G. Klärner, B. Krawczyk, V. Ruster, U. K. Deiters, *J. Am. Chem. Soc.* **1994**, *116*, 7646−7657.
[30] J. J. Bloomfield, J. S. McConaghy, *Tetrahedron Lett.* **1969**, 3723−3726.
[31] R. S. H. Liu, *J. Am. Chem. Soc.* **1967**, *89*, 112−114.
[32] K. M. Schumate, P. N. Neuman, G. J. Fonken, *J. Am. Chem. Soc.* **1965**, *87*, 3996.
[33] A. Padwa, W. Koehn, J. Masaracchia, C. L. Osborn, D. J. Trecker, *J. Am. Chem. Soc.* **1971**, *93*, 3633−3638.
[34] J. R. Wiseman, F. P.-K. Liu, W. M. Butler, *193rd National Meeting of the American Chemical Society, Denver, CO*, April **1987**, ORGN 152.
[35] F. P.-K. Liu, Ph.D. Thesis, The University of Michigan, **1987** (Director: J. R. Wiseman).
[36] R. B. Woodward, R. Hoffmann, *Angew. Chem.* **1969**, *81*, 797−869; *Angew. Chem. Int. Ed. Engl.* **1969**, *8*, 781−853.
[37] R. B. Woodward, R. Hoffmann, *The Conservation of Orbital Symmetry*, Academic Press, New York, **1970**; *Die Erhaltung der Orbitalsymmetrie*, Verlag Chemie, Weinheim, **1972**.
[38] W. R. Roth, V. Paschmann, *Liebigs Ann.* **1996**, 1329−1336.
[39] W. R. Roth, F. Hunold, *Liebigs Ann.* **1996**, 1917−1928.
[40] W. R. Roth, T. Bastigkeit, *Liebigs Ann.* **1996**, 2171−2183.
[41] W. R. Roth, R. Gleiter, V. Paschmann, U. E. Hackler, G. Fritzsche, H. Lange, *Eur. J. Org. Chem.* **1998**, 961−967.
[42] J. Leitich, *Tetrahedron* **1982**, *38*, 1303−1309.
[43] Rate constants for dimerisation refer to the rate of *reaction* (rather than to the rate of disappearance of **9**) while dimer concentrations such as [**11**] refer to C_8 units. This entails a factor of 2 in the rate equations: $d[\mathbf{11}]/dt = 2k_{\mathbf{11}}[\mathbf{9}]^2$. All error limits in this work refer to a probability level $P = 0.95$.
[44] The dimerisation rate constants reported in ref.[33], after dividing by 60 to convert minutes to seconds, are still higher by orders of magnitude than the ones we determined in cyclohexane and *n*-octane as the solvents, which would entail a gross discrepancy between the $\Delta S^{\ddagger}$ value determined in ref.[33] (−10 eu) and the one that we determined (−33.5 eu). On the other hand, the *relative* rate constants at different temperatures are similar to ours, resulting in an activation energy in fair agreement with that determined by us. Since the discrepancy is far beyond experimental error we suspect a systematic clerical error in the determination of the rate constants reported in ref.[33]
[45] J. Chateauneuf, J. Lusztyk, K. U. Ingold, *J. Org. Chem.* **1988**, *53*, 1629−1632.
[46] A. L. J. Beckwith, V. W. Bowry, K. U. Ingold, *J. Am. Chem. Soc.* **1992**, *114*, 4983−4992.
[47] V. W. Bowry, K. U. Ingold, *J. Am. Chem. Soc.* **1992**, *114*, 4992−4996.
[48] I. W. C. E. Arends, P. Mulder, K. B. Clark, D. D. M. Wayner, *J. Phys. Chem.* **1995**, *99*, 8182−8189.
[49] R. Huisgen, *Acc. Chem. Res.* **1977**, *10*, 117−124.
[50] The *conjugated* 1,4-diradical that is intermediate in the course of the thermal [2+2] cyclodimerisation of an allene has been successfully trapped by nitroxyl with formation of 2:2 adducts: A. T. Bottini, L. J. Cabral, V. Dev, *Tetrahedron Lett.* **1977**, 615−618.
[51] An unconjugated singlet bis(allylic) 1,5-diradical has been found to undergo efficient trapping with dioxygen.[41]
[52] In a thermolysis system homologous with that displayed in Scheme 2, trapping of the intermediate singlet bis(allylic) 1,4-diradical by dioxygen appears to have been observed: W. R. Roth, unpublished, cited in ref.[53]
[53] W. v. E. Doering, J. L. Ekmanis, K. D. Belfield, F.-G. Klärner, B. Krawczyk, *J. Am. Chem. Soc.* **2001**, *123*, 5532−5541.
[54] B. Maillard, K. U. Ingold, J. C. Scaiano, *J. Am. Chem. Soc.* **1983**, *105*, 5095−5099.
[55] A. Marchaj, D. G. Kelley, A. Bakac, J. H. Espenson, *J. Phys. Chem.* **1991**, *95*, 4440−4441.
[56] R. Zils, S. Inomata, Y. Okunuki, N. Washida, *Chem. Phys.* **1998**, *231*, 303−313.
[57] A. R. Costello, J. R. L. Smith, D. J. Waddington, *Int. J. Chem. Kinet.* **1996**, *28*, 201−215.
[58] H. Dilger, M. Stolmar, P. L. W. Tregenna-Piggott, E. Roduner, I. D. Reid, *Ber. Bunsenges. Phys. Chem.* **1997**, *101*, 956−960.
[59] H. Dilger, M. Schwager, P. L. W. Tregenna-Piggott, E. Roduner, I. D. Reid, D. J. Arseneau, J. J. Pan, M. Senba, M. Shelley, D. G. Fleming, *J. Phys. Chem.* **1996**, *100*, 6561−6571.
[60] V. D. Knyazev, I. R. Slagle, *J. Phys. Chem.* **1995**, *99*, 2247−2249.

[61] F. F. Fenter, B. Noziere, F. Caralp, R. Lesclaux, *Int. J. Chem. Kinet.* **1994**, *26*, 171−189.
[62] O. Dobis, S. W. Benson, *J. Am. Chem. Soc.* **1993**, *115*, 8798−8809.
[63] L. Elmaimouni, R. Minetti, J. P. Sawerysyn, P. Devolder, *Int. J. Chem. Kinet.* **1993**, *25*, 399−413.
[64] A. J. McLean, M. A. J. Rodgers, *J. Am. Chem. Soc.* **1993**, *115*, 4786−4792.
[65] J. A. Berson, P. B. Dervan, R. Malherbe, J. A. Jenkins, *J. Am. Chem. Soc.* **1976**, *98*, 5937−5968.
[66] K. Gundertofte, T. Liljefors, P.-O. Norby, I. Pettersson, *J. Comp. Chem.* **1996**, *17*, 429−449.
[67] Cobaltocene is known to add to carbon-centred free radicals: J. E. Sheats, *J. Organomet. Chem. Libr. (Organomet. Chem. Rev.)* **1979**, *7*, 461−521.
[68] J. C. Calvert, J. N. Pitts, Jr., *Photochemistry*, John Wiley, New York, **1966**, p. 304 ff.
[69] G. L. Lange, E. Neidert, *Can. J. Chem.* **1973**, *51*, 2207−2214.
[70] P. E. Eaton, K. Lin, *J. Am. Chem. Soc.* **1964**, *86*, 2087−2088.
[71] J. Leitich, H. Sprintschnik-Krenn, I. Heise, unpublished results.
[72] C. Krüger, unpublished results.
[73] V. Rautenstrauch, *Helv. Chim. Acta* **1973**, *56*, 2492−2508.
[74] A. C. Cope, C. L. Bumgardner, *J. Am. Chem. Soc.* **1956**, *78*, 2812−2815.
[75] R. M. Manyik, F. C. Frostick, J. J. Sanderson, C. R. Hauser, *J. Am. Chem. Soc.* **1953**, *75*, 5030−5032.
[76] A. K. Hoffmann, A. M. Feldman, E. Gelblum, A. Henderson, *Org. Synth.* **1968**, *48*, 62−64.
[77] R. T. Major, *J. Am. Chem. Soc.* **1931**, *53*, 4373−4378.
[78] G. Kresze, G. Schulz, *Tetrahedron* **1961**, *12*, 7−12.
[79] R. H. Shapiro, *Org. React.* **1967**, *23*, 405−507.
[80] D. H. R. Barton, V. N. Le Gloahec, J. Smith, *Tetrahedron Lett.* **1998**, *39*, 7483−7486.
[81] G. M. Sheldrick, *SHELXS-97, Program for the determination of crystal structures*, University of Göttingen, Germany, **1997**.
[82] G. M. Sheldrick, *SHELXL-97, Program for least-squares refinement of crystal structures*, University of Göttingen, Germany, **1997**.

Received December 5, 2001
[O01572]